Analysis of Lipid Biomarker Composition and Distribution Across the Salinity Gradient of the Manialtepec Lagoon, Mexico

-William O. Jordan-

Master's Thesis

Supervisors:
Pablo Martínez-Sosa
Francien Peterse

Utrecht University, Faculty of Geosciences
Department of Earth Sciences: Earth, Life and Climate
The Netherlands
30-05-2024

Contents

Abstract

Estuaries play an important role in the global carbon cycle. Roughly 0.4 Pg of terrestrial organic matter (terrOM) is transported through fluvial systems into the oceans, but only around 0.1-0.2 Pg of it is eventually buried in marine sediments. This indicates that roughly 50-75% of the terrOM is removed from the water whilst travelling through estuaries. However, the carbon sources and sinks within the estuaries are not understood very well.

Past studies have shown that there are many processes that change the composition and distribution of terrOM throughout the estuary. These processes include microbial degradation, in situ carbon prodution, mineralisation, flocculation, and photochemical oxidation. It is however not fully understood how salinity gradients in estuaries affect the terrOM. Analysis on bulk dissolved OM has shown that OM is immobilized due to mineral-OM interactions at higher salinities, but also that ligand and ion exchange compete with the immobilization process causing higher OM degradation at higher salinities.

In this work we apply a biomarker-focused approach to study the flux of organic matter the Manialtepec lagoon, located on the Pacific coast of Mexico. This lagoon is supplied fresh water through the Manialtepec river and is protected from the ocean by a sandbank during the dry season. However, during the wet season saline ocean water is able to enter into the lagoon through two openings that appear in the sandbank. As a result of the different phases in water supply, a strong salinity gradient is present throughout the lagoon. By analysing the biomarkers organic matter changes at molecular level could become clear through a transect of the estuary.

Using fatty acid (FA) and glycerol dialkyl glycerol tetraether (GDGT) biomarkers and paleoenvironmental indices, such as the BIT-index, it was found that ecological niches determine the fate of OM in an estuary. Evidence of microbial communities were found in the fresh water section and salt water section of the estuary. At the fresh-salt water interface a change in ecological niche was detected, as different biomarker signatures were found in the river and lagoon. Also, terrestrial biomarkers were found in the sediment layer and not in the water column, as a result of sequestering and microbial reworking. It was concluded that estuaries rework terrestrial OM strongly, after which only small amounts enter the open ocean, or it enters the ocean as aquatic OM.

1 Introduction

1.1 Background

With global CO_2 emissions increasing due to the burning of fossil fuels for transportation and industry for instance, it becomes increasingly important to better understand the global carbon cycle (Jackson et al., 2017). Higher global CO_2 concentrations in the atmosphere result in a stronger global greenhouse effect and subsequently warms the planet to unnatural levels (Anderson et al., 2016). The higher global temperature has catastrophic implications on the climate. For example, effects of an increased global temperature, such as extreme weather and rising sea levels from melting ice caps would become very dangerous for human life. However, carbon on earth is distributed unbalanced between terrestrial, aquatic, and atmospheric reservoirs. Many uncertainties exist around the size of these reservoirs, and especially the size of the fluxes between them (Cole et al., 2007). Many processes can act as carbon sources or sinks for each reservoir, complicating the calculation of carbon fluxes. Also, many of the carbon sinks will eventually turn in to a carbon source, but it is difficult to predict when this change will occur in the future.

A way to elucidate the cycling of carbon through the Earth's system is by identifying and researching the size and importance of major carbon sources and sinks. For instance, organic matter (OM) produced when terrestrial organisms capture CO_2 from the atmosphere can eventually enter soils or the fluvial environment where it can then be transported to the marine environment through fluvial systems. It is also possible for the terrestrial organic matter (terrOM) to be buried in riverbank deposits or be recycled by aquatic microbes after which the carbon returns to the atmosphere as CO_2. Riverbank deposits and microbial recycling of OM are examples of short-term carbon sinks in the fluvial systems. The transitional system between terrestrial and marine reservoirs is of major importance to the global carbon cycle as it can also lead to a long-term carbon sink. Roughly one third of the terrOM that is transported through fluvial systems to the oceans is assumed to be eventually buried in marine continental shelves, in particular deltaic sediments (Burdige, 2005). The terrOM that is buried in the sediments on the continental margins is assumed to stay there a for long time. As a result, this type of burial in the marine sediments acts as a long-term carbon sink.

In a previous study it was estimated that yearly 0.25 Pg (1 Pg = 1×10^{15} g) of Dissolved OM (DOM) and 0.15 Pg of Particulate OM (POM) is discharged through fluvial systems into to the ocean (Hedges et al., 1997). Of this it is estimated that only 0.1-0.2 Pg carbon is buried in marine sediments. This indicates that around 50%-75% of the terrOM is removed from the system whilst being transported through the estuaries before entering the marine environment, or it is recycled in the marine water column and never reaches the sediment layer. However, the carbon sources and sinks in these transitional coastal areas are very difficult to quantify for a total carbon budget (Bauer et al., 2013). This is due to large diversity within the biogeochemical processes that influence the fate of OM in estuaries. Natural and anthropogenic processes change the fluxes of OM from riverine systems in to coastal oceans. Examples of anthropogenic processes are agricultural nutrient input to soil or soil disturbance, as well as the artificial change of the hydrology of estuarine environments by placing dams and removing wetlands. Natural processes range from physiological effects, such as flocculation and sedimentation, to more biological examples, for instance primary production and microbial recycling of OM. With so many possible biogeochemical processes regulating the fate of the OM, the uncertainties within known carbon cycle models (used in, eg. Burdige, 2005, Aufdenkampe et al., 2011, Bauer et al., 2013) become increasingly larger.

Next, some of the many biogeochemical processes present in an estuary that can act as possible carbon sources and sinks will be highlighted. These processes are also depicted as a schematic in Figure 1. As terrOM enters the estuary through fluvial transportation it can be decomposed by oxidising processes to CO_2 and thus being returned into the atmosphere as gas. The terrOM can also sink towards the sediment layer of the estuary or open ocean when it is buried, which is considered a long term sink of OM. The oxidative decomposition of OM and OM burial are examples of important processes on the carbon fluxes between the three major reservoirs (Repasch et al., 2021). However, the terrOM is also modified whilst remaining in the water column. Examples of these processes are in situ primary production, mineralisation, flocculation, microbial degradation, and photochemical changes.

In situ primary production acts as a source of new OM in estuaries. Here dissolved CO_2 is taken by algae and cyanobacteria and new DOM and POM is produced, but also existing OM is reworked by microbes. On the other hand, microbial degradation and photochemical oxidation are examples of carbon sinks from the estuary. In both processes OM is degraded to CO_2 which is released back into the atmosphere. However, with microbial degradation the OM is oxidized with O_2 as a reducing agent, whereas with photochemical oxidation the reaction is driven by energy obtained from incoming light (Bauer et al., 2013).

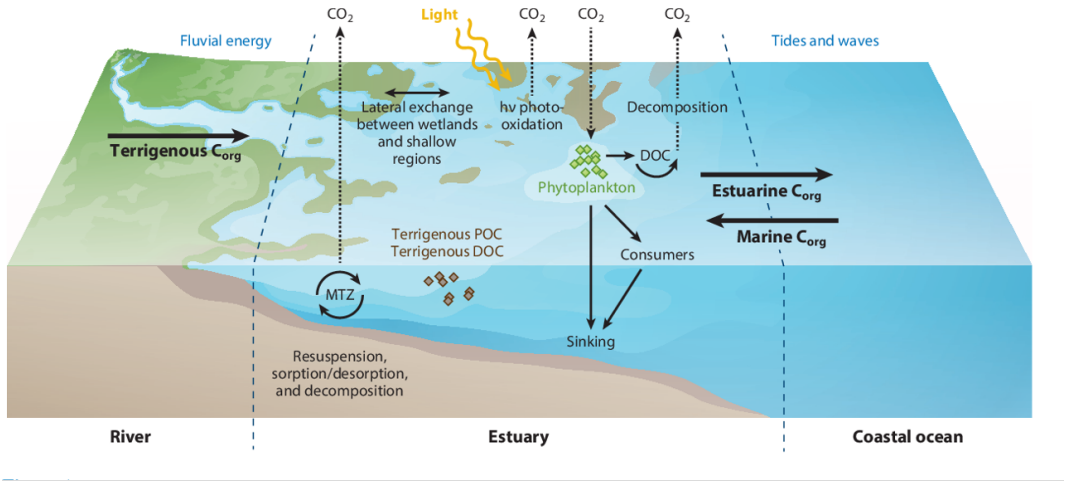

Figure 1: Schematic depicting the most important biogeochemical processes of organic matter (abbriviated as OC in the image) that occur in an estuary. Image was taken from Canuel and Hardison, 2016.

With processes such as microbial respiration and degradation, acting as non-reversible sources or sinks of OM and CO_2 in estuaries, there are also many processes that do not add or remove OM to the system. Rather, these processes change the distribution of the OM using a reversible mechanism. An example of one of these reversible processes is flocculation. With flocculation DOM aggregates in the water and forms POM, thus not removing the OM from the water. The newly formed POM could however sink down the water column and eventually be buried in sediments resulting in a sink. But, often the POM remains suspended in the water column.

Similarly, minerals in soils can form bonds and interact with the OM, immobilising it. The immobilised OM therefore becomes protected from further degradation, when entering a river for instance (Gao et al., 2020). The mineral-OM interaction is thought to occur through multi-layer adsorption conceptualised in a model by Kleber et al., 2007. In the first layer, the polar functional groups of the OM bond with hydroxyl groups on the mineral surface. The second layer arises as a membrane-like bi-layer where hydrophobic parts of organic compounds face the mineral surface and the hydrophilic groups are pointed towards the aqueous solution. Lastly, in the third layer more organic compounds are able to form interactions with the hydrophilic groups present in the second membrane-like layer. Examples of interactions in the final layer of the adsorption model are hydrogen bonding and ion-ion interactions.

OM in soils and water is vastly complex and is made by many different producers. As the OM is exposed to many degradation methods it becomes important to know what implications these may have on it. For example, in the ocean there are many primary producers who take up organic carbon, such as algae and bacteria (Lee et al., 2004). These organisms produce various detectable hydrocarbon compounds, including carbohydrates, solvent extractable lipids, amino acids, and pigments such as chlorophyll. Structures and functional groups differ between the hydrocarbon compounds. Amino acids contain high percentages of nitrogen and carbon when measured for instance. Also, the chemical composition can vary through what functional group is present, such as hydroxyl, carbonyl, or

aromatic groups (Chen et al., 2002). These differences in structure and chemical composition strongly influence the lability of the OM. All the biogeochemical processes mentioned earlier can change the chemical composition of the existing OM. Labile organic compounds are prone to fast degradation and therefore become undetectable. The degraded OM falls outside of the analytical window of the available analytical methods, such as chromatography and spectroscopy (Lee et al., 2004). It becomes very difficult to determine the biological source or the eventual fate of OM when it is heavily degraded.

The influence of salinity changes on the composition and distribution of OM across the estuary is relatively unknown (Osterholz et al., 2016). Nevertheless, it is a potentially important factor. Since, due to mixing of fresh fluvial water and saline marine water a strong salinity gradient is present along the course of all estuaries. It is thought that changes in salinity could have a particularly important effect on the mineral-organic matter interactions. Previous work has shown that, at higher salinities, OM is immobilized through Van der Waals interactions with mineral surfaces, and thus protected from degradation. However, interactions such as ligand and ion exchange with competing ions and mineral surfaces, or hydrogen bonding have also been shown to have the opposite effect, potentially increasing the degradation of OM (Kida & Fujitake, 2020). Having competing processes across the salinity gradient of an estuary, it becomes more difficult to thoroughly understand the fate of the OM in the estuaries.

In previous studies (eg. Kida and Fujitake, 2020, Middelburg and Herman, 2007, Osterholz et al., 2016) bulk OM in the water has been analysed. They found that OM is immobilised in waters with higher salinities and therefore is more protected from oxidation and photodegradation. Also, physical characteristics of the estuary, such as water residency time and incoming light levels, have great impact on the degradation of DOM. However, since these studies focus on bulk characteristics, it is not possible to obtain resolution at the molecular level (Hedges et al., 1997, Cole et al., 2007).

Knowing what happens to OM on a molecular level is of great importance to approach more exact carbon fluxes between terrestrial, aquatic, and atmospheric reservoirs (Hedges et al., 1997). By analysing samples across an estuary at a molecular scale, rather than bulk, the fate of specific organic compounds can be determined. As well as providing an insight into important biogeochemical processes (Meyers & Ishiwatari, 1993). To accomplish the molecular analysis, compounds must maintain analysable functional groups over a longer period of time, thus being recalcitrant (Brocks et al., 2005). One type of recalcitrant molecules are membrane lipids. Membrane lipids are produced by all living organisms and can be found ubiquitously on earth. Some of these membrane lipids have the unique property of only being produced by specific organisms (Peters et al., 2005). These recalcitrant source-specific membrane lipids are often used as an indicator for biological activity and geological processes. When used as an indicator the membrane lipids are referred to as lipid biomarkers.

Lipid biomarkers are present and preserved in soils, sediments, rocks, and water and they can provide important climatic and environmental information. Environmental parameters, such as temperature, salinity, and pH strongly influence the chemical structure of lipid biomarkers (Summons et al., 2022). There are many types of biomarker molecules used to identify OM, including alkanes, sterols, and fatty acids. Two important lipid biomarkers used in the assessment of carbon cycles are Fatty Acids (FAs) and Glycerol Dialkyl Glycerol Tetraethers (GDGTs) (Rustan and Drevon, 2001, Schouten et al., 2002). By analysing their composition and distribution throughout the estuary important biogeochemical processes of OM are illustrated. For this, analysis of individual FA and GDGTs is performed, but also proxies have been determined to exhibit environmental parameters influences on membrane lipid production (eg. Volkman et al., 1980, Wang and Liu, 2012, Gliozzi et al., 1983). With biomarker analysis more information can be gained on the fate of OM travelling through estuaries from terrestrial environments (W. Guo et al., 2019). In Section 1.2.1 a detailed explanation on how FAs and GDGTs are used. And how corresponding environmental indices are implemented to determine the sources of OM and associated biogeochemical processes in an estuary.

1.2 Using lipid biomarkers for carbon transport analysis

1.2.1 Fatty acids as lipid biomarkers

Fatty acids (FAs) are lipids that are present in cells and contribute strongly to key roles in metabolism, such as energy storage and membrane structuring (Harwood & Gurr, 2013). FAs are molecules that are very diverse in structure (Rustan & Drevon, 2001). The FA molecules are built up from a carbon chain that contains a methyl group at one end, and a carboxyl group (-COOH) at the other end. The carbon chain in between the methyl and carboxyl moieties can vary in length and degree of saturation.

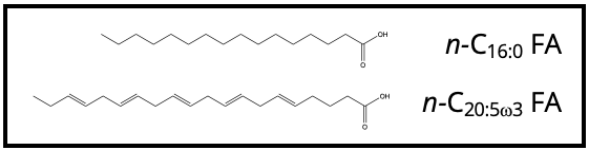

Figure 2: Two examples of the structure of fatty acid biomarkers and their names. The carbon chain length is indicated with the first number in subscript (top: 16, lower: 20) and the amount of double bonds is indicated with the second number in the subscript (top: 0, lower: 5). The ω3-notation indicates that the first double bond is located between C_3 and C_4 counting from the methyl end member.

Saturated FAs are straight chained and contain no double bonds. Opposingly, unsaturated FAs are not straight chained and contain double bonds between two carbon atoms, resulting in a loss of two hydrogen atoms per double bond. When naming FAs the carbon atom in the end membered methyl group is indicated with an omega (ω) symbol, and the carbon atom connected to carboxyl moiety is named the alpha (α) carbon. The FAs are subsequently named by how many carbon atoms the chain contains, and the number of double bonds present in the chain. For example, a straight chain FA containing 18 carbon atoms is referred to as $C_{18:0}$. A FA that contains the same amount of carbon atoms but has a double bond on the third carbon from the ω-position is called $C_{18:1\omega3}$. This systematic numerical nomenclature is used for FAs of all different chain lengths. The structure of $C_{16:0}$ and $C_{20:5\omega3}$ are shown in Figure 2 as examples.

Certain FAs are produced by specific organisms and can therefore be used as an indicator or biomarker. By analysing FAs that show conservative behaviour over time and that are source specific, OM matter sources and biogeochemical processes can be identified (Sargent, 1987, Meyers and Ishiwatari, 1993, Holtvoeth et al., 2010). Different microbial sources of FAs in the Manialtepec system include bacteria, algae, and phytoplankton. First, we will discuss which FAs are indicative of microbial sources.

Bacterial communities are known to produce low molecular weight (LMW), with chains between 12 and 20 carbon atoms long (nC_{12-20}), odd carbon numbered saturated FAs. Additionally, $C_{15:0}$ and $C_{17:0}$ branched FAs (iso and anteiso), as well as the mono unsaturated FA (MUFA) $C_{18:1\omega7}$ are produced by bacteria (Volkman et al., 1980, Parkes and Taylor, 1983, Meziane and Tsuchiya, 2000). As these FAs are ubiquitous in bacteria, they cannot be used to highlight individual bacterial species, but rather indicate the presence of bacteria in general. An FA profile containing predominantly $C_{16:0}$, $C_{16:1\omega7}$, $C_{18:2\omega6}$, and $C_{18:3}$ as the most common poly unsaturated fatty acid (PUFA) is indicative of a cyanobacterial presence in the system (Ahlgren et al., 1992).

LMW even carbon numbered FAs are indicative of microalgae and phytoplankton. Predominantly $C_{14:0}$, $C_{16:0}$, and $C_{18:0}$ are reported to be found in phytoplankton communities (Wakeham, 1985). The MUFAs $C_{16:1\omega7}$, $C_{18:1\omega7}$, and $C_{18:1\omega9}$, as well as the PUFA $C_{20:5\omega3}$, and $C_{22:6\omega3}$ are also used to detect phytoplankton (Napolitano, 1999). The most common group of phytoplankton in marine environments are diatoms and dinoflagellates. The PUFAs $C_{20:5\omega3}$ and $C_{22:6\omega3}$ are commonly used as biomarkers for diatoms and dinoflagellates respectively (Nichols et al., 1983, Lowe et al., 2014).

Other sources that can be determined by FAs are those derived from terrestrial vascular plants. Wax coatings of plant leaves and flowers contain high amounts of long chain FAs (LCFA). The LCFAs that are reported as being connected to these vascular plants are fully saturated with an even carbon chain of $>C_{20}$ (Volkman and Johns, 1977, Matsuda and Koyama, 1977). The presence of $>C_{20}$ in aquatic and

sediment samples are an indication of terrestrial input in the system. Furthermore, terrestrial higher plants and mangroves produce the PUFAs $C_{18:2\omega6}$ and $C_{18:3\omega3}$ (Budge and Parrish, 1998, Dalsgaard et al., 2003).

Several indices have been suggested to distinguish OM sources from each other, using relative ratios of FAs. An important ratio to determine if OM is from a terrestrial or a marine source is the Average Chain Length (ACL) (Wang and Liu, 2012, Fang et al., 2014). The FA ACL is calculated with Equation 1.

$$\mathrm{ACL}_{16-32} = \frac{\Sigma C_i \cdot i}{\Sigma C_i} \tag{1}$$

Here Ci is the concentration of a fatty acid containing i amount of carbons in its chain. Wang and Liu, 2012 found that when using saturated FAs with an even number of carbon atoms ranging from C_{16} to C_{32} in the ACL, the indicator can be used to discriminate between aquatic and terrestrial inputs. Consequently, an ACL that is smaller than 18.6 indicates a predominantly marine input to the system, and an ACL that is greater than 23.3 indicates more terrestrial input.

1.2.2 Glycerol dialkyl glycerol tetraethers as lipid biomarkers

Glycerol Dialkyl Glycerol Tetraethers (GDGTs) are membrane stretching biomarker lipids produced by archaea (De Rosa & Gambacorta, 1988) and some bacteria (Weijers, Schouten, Hopmans, et al., 2006). GDGTs are built up by two long alkyl chains that are connected by glycerol heads at the ends of each chain (Chappe et al., 1979). They have been abundantly found in soils (Weijers et al., 2007), rivers (Kirkels et al., 2020), and lacustrine sediments (Baxter et al., 2021), as well as marine water columns and marine sediments (Schouten et al., 2002), and can be used as environmental indicator. The GDGT biomarkers can be characterised in two main groups, namely isoprenoid and branched. GDGTs are relatively recalcitrant molecules that are not subjected to degradation over many years. Also, they contain information on environmental parameters, such as temperature and pH. Therefore, GDGTs can be used for paleoclimatic reconstructions and analysis on biogeochemical cycles in a complex system, such as an estuary.

1.2.3 isoGDGTs

Isoprenoid GDGTs (isoGDGTs) are produced by archaea and it is presumed they are mainly produced in marine environments (Schouten et al., 2002). The alkyl chains for isoGDGTs are built up from isoprene molecules, resulting in two isoprenoid alkyl chains present in an isoGDGT molecule. The alkyl chains can also contain cyclopentane rings in varying quantities, ranging from zero to eight, divided over the two alkyl chains. IsoGDGTs are named GDGT-0 through GDGT-8 depending on how many cyclopentane rings are present in the molecule. A unique isoGDGT is crenarchaeol (cren) and its regio-isomer (cren')(Damsté et al., 2002). Cren and cren' are biomarker lipids that can be specifically attributed to *Traumarchaeota*, which are a phylum of archaea. (Pitcher et al., 2011). The molecules contain four cyclopentane rings, but have an additional cyclohexane moiety present in one of the alkyl chains. In Figure 3A the most common isoGDGT (0-3) and crenarchaeol structures are shown.

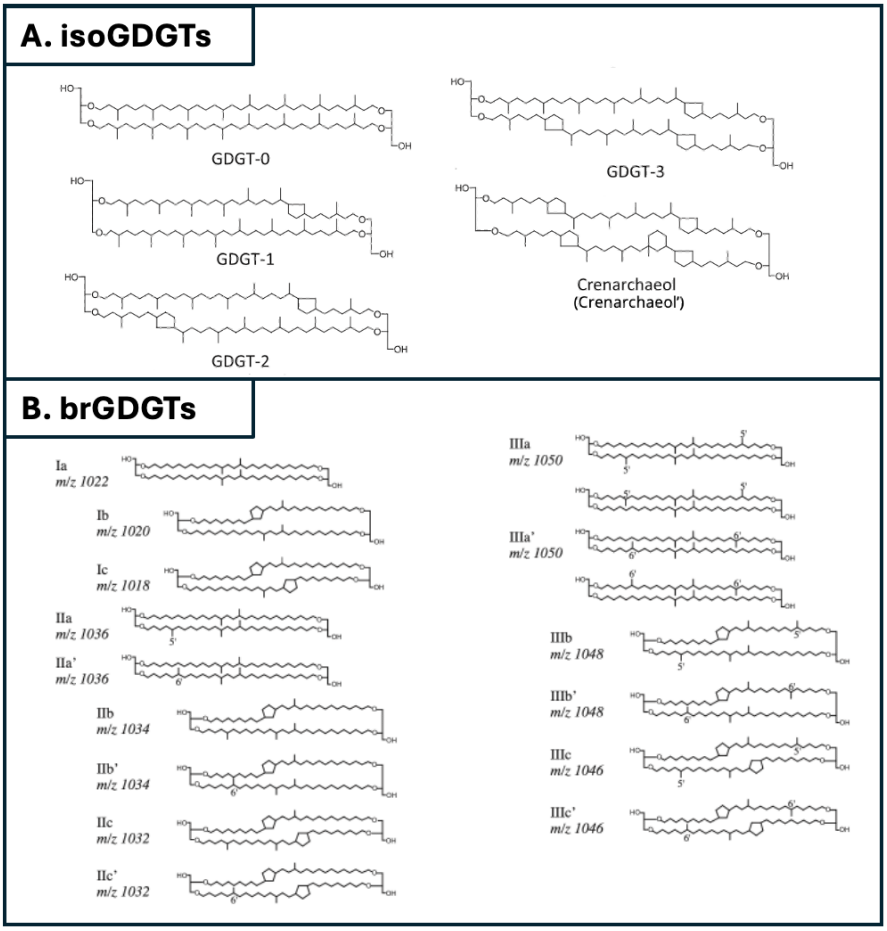

Figure 3: A. Chemical structures of the most common isoprenoid GDGTs used in environmental proxies. The figure shows structures for GDGT-0 to GDGT-3 and crenarchaeol (figure adapted from Schouten et al., 2013), B. Chemical structures of the most common branched GDGTs in environmental proxies. Ia, IIa, and IIIa are the brGDGTs with 0 cyclopentane moieties. The respective b and c notation indicate 1 or 2 cyclopentane moieties in the molecule. The prime notation (eg. IIa') indicates the 6-methylated isomer of the brGDGT (figure adapted from De Jonge, Stadnitskaia, et al., 2014)

Previous studies have shown a positive correlation between the amount of cyclopentane rings present in an isoGDGT with a higher environmental temperature (Gliozzi et al., 1983, De Rosa et al., 1986). This observation led to the development of a sea surface temperature (SST) based proxy using relative abundances of isoGDGTs. The TetraEther index consisting of 86 carbons (TEX_{86}) was introduced by Schouten et al., 2002 as proxy, and has been used as an indicative paleothermometer of SST (Eq. 2).

$$TEX_{86} = \frac{[\text{GDGT-2}]+[\text{GDGT-3}]+[\text{cren'}]}{[\text{GDGT-1}]+[\text{GDGT-2}]+[\text{GDGT-3}]+[\text{cren'}]} \quad (2)$$

TEX_{86} values are calculated by taking the relative abundance of the sum of GTGT-2, GDGT-3, and cren' and the sum of GDGT-1, GDGT-2, GDGT-3, and cren'. When isoGDGTs with more cyclopentane rings are present in a sample, higher TEX_{86} values will be calculated. Therefore, higher TEX_{86} values correspond to higher SSTs. A calibration of the TEX_{86} index was performed by analysing a widely spread, global core top data set, which showed a linear correlation between TEX_{86} values and SST between a range of 5 to 30°C (Kim et al., 2008).

Additionally, isoGDGTs are also used in another environmental proxy to indicate the influence of methanogenic archaea. Methanogenic archaea are known to produce higher concentration of GDGT-0 to GDGT-3 in lacustrine settings compared to the other isoGDGTs (Sinninghe Damsté et al., 2001).

By taking the ratio between the relative abundance of methanogen produced GDGT over that produced in marine conditions, the influence of Methanogenesis on GDGT distribution can be expressed. The Methanogenesis is calculated with Equation 3.

$$\text{Methanogenesis} = \frac{[\text{GDGT-0}]}{[\text{cren}]} \tag{3}$$

In the Methanogenesis proxy only GDGT-0 is used to determine the influence of Methanogenesis, as it has been found that methanogens dominantly produce GDGT-0 (Blaga et al., 2009). GDGT-1, GDGT-2, and GDGT-3 are also produced by methanogens, but also by anaerobic methane oxidising archaea. Therefore they are not considered when determining the Methanogenesis input, as the shared source of those isoGDGTs could result in an overestimation of methanogens (Sinninghe Damsté et al., 2001, Blumenberg et al., 2004). A substantial methanogenic input for GDGT-0 is presumed when the calculated ratio is >2 (Blaga et al., 2009).

1.2.4 brGDGTs

Branched GDGTs (brGDGTs) are produced by bacteria and are mainly found in terrestrial material, such as soils (Weijers, Schouten, Spaargaren, & Damsté, 2006) and peats (Weijers, Schouten, Hopmans, et al., 2006). The brGDGTs contain alkyl chains that are branched with methyl groups and cyclopentane rings. The most common brGDGTs have four, five, or six methyl groups present on the alkyl chain, as well as up to two cyclopentane moieties. The names for the brGDGTs are Ia, IIa, and IIIa for the tetra, penta, and hexa methylated brGDGTs respectively. The letters a, b, and c indicate if the molecule has zero, one, or two cyclopentane moieties. The cyclopentane moieties are in the position of a methyl group on the alkyl chain. The additional methyl groups in II and III can be located on the 5 or 6 position from the glycerol ends, resulting in two different isomers. In naming the 6-methyl isomer a prime (') symbol is added to the numbering, for instance IIa' (De Jonge, Stadnitskaia, et al., 2014). The structures of these brGDGTs are displayed in Figure 3B.

Comparably to isoGDGTs, the cyclisation, isomerisation, and methylation of brGDGTs correlate well with environmental parameters, such as temperature and pH. One environmental proxy based on brGDGTs is the Cyclisation index of Branched Tetraethers (CBT)(Eq. 4)(Weijers et al., 2007).

$$\text{CBT} = \text{-log}\frac{[\text{Ib}]+[\text{IIb}]}{[\text{Ia}]+[\text{IIa}]} \tag{4}$$

$$\text{CBT} = 3.33 - 0.38 \cdot \text{pH} \tag{5}$$

The CBT is used to measure the degree of cyclisation (amount of cyclopentyl moieties) in brGDGTs. For this, a ratio is taken between the sum of Ib and IIb over Ia and IIa. The other brGDGTs are not considered in the ratio as they are often only present in low abundances (Weijers et al., 2007). The index is defined as a negative log, which results in a positive correlation between the CBT and pH values (Eq. 5). At lower CBT values the brGDGTs were produced in an environment with lower pH values.

The Methylation index of Bracnched Tetraethers (MBT) is a second environmental proxy using brGDGTs (Weijers et al., 2007). This proxy is used to highlight the correlation between the degree of methylation of brGDGTs and temperature. It is implemented broadly for paleo-climatic reconstructions, similarly to TEX_{86}, but instead of SST it is used for Mean Annual air Temperature (MAT) reconstruction.

$$\text{MBT} = \frac{[\text{Ia}]+[\text{Ib}]+[\text{Ic}]}{[\text{Ia}]+[\text{Ib}]+[\text{Ic}]+[\text{IIa}]+[\text{IIb}]+[\text{IIc}]+[\text{IIIa}]+[\text{IIIb}]+[\text{IIIc}]} \tag{6}$$

$$\text{MBT} = 0.867 + 0.096 \cdot \text{pH} + 0.021 \cdot \text{MAT} \tag{7}$$

As shown in Equation 6 higher MBT values are the result of a larger relative abundance of the tetra methylated brGDGTs (Ia, Ib, Ic). Weijers et al., 2007 found a relationship between MAT and MBT, as shown in Equation 7.

Equations 4 and 6 were developed when GDGT separation techniques did not separate the 5 and 6-methylated brGDGTs. After Hopmans et al., 2016 introduced a new chromatographic method for GDGT analysis where the two isomers eluded separately, the CBT and MBT indices were rewritten to include the 5 and 6-methyl isomers individually. However, De Jonge, Hopmans, et al., 2014 found that the concentration of 6-methyl isomers of various brGDGTs showed strong correlation with one another, it was assumed they were produced by a common source. Therefore, the 6-methyl isomers were removed from the equations to prevent over representation of the 6-isomer, and the indices were rewritten to CBT'$_{5Me}$ (Eq. 8) and MBT'$_{5Me}$ (Eq. 9) (De Jonge, Hopmans, et al., 2014). The new indices result in more accurate climate reconstructions, as the correlation errors are reduced by the removal of the common-source 6-methyl isomers.

$$\text{CBT'}_{5\text{Me}} = \text{-log}\frac{[\text{Ib}]+[\text{IIb}]}{[\text{Ia}]+[\text{IIa}]} \tag{8}$$

$$\text{MBT'}_{5\text{Me}} = \frac{[\text{Ia}]+[\text{Ib}]+[\text{Ic}]}{[\text{Ia}]+[\text{Ib}]+[\text{Ic}]+[\text{IIa}]+[\text{IIb}]+[\text{IIc}]+[\text{IIIa}]+[\text{IIIb}]+[\text{IIIc}]} \tag{9}$$

Another environmental, GDGT-based proxy is the Branched Isoprenoid Tetraether (BIT) index, which combines both iso- and brGDGTs (Hopmans et al., 2004). The BIT index is used to discern a difference between marine and terrestrial environmental inputs. It is based on the findings that isoGDGTs are mainly produced by marine archaea and brGDGTs by bacteria in terrestrial systems. By comparing the relative abundance of brGDGTs to that of the Thaumarchaeota-produced isoGDGT chrenarchaeol, the BIT-index is calculated (Eq. 10).

$$\text{BIT} = \frac{[\text{Ia}]+[\text{IIa}]+[\text{IIIa}]}{[\text{cren}]+[\text{Ia}]+[\text{IIa}]+[\text{IIIa}]} \tag{10}$$

To calculate the BIT-indedx only the brGDGTs Ia, IIa, and IIIa and the isoGDGT crenarchaeol are used. Higher BIT values indicate a larger relative abundance of brGDGTs, thus more terrestrial input in the system. For lower BIT values the opposite is true, as a larger relative abundance of crenarchaeol shows a more marine input into the system.

1.3 Manialtepec Lagoon

The Manialtepec Lagoon is a saline lagoon located on the south coast of Mexico in the state of Oaxaca (Fig. 4A). Here the tropical temperatures almost remain constant throughout the year, with monthly average temperatures ranging between 26°C and 28°C. The year is divided into two seasons: wet and dry. The wet season is between the months May and November and an average of around 380 mm of rain falls per month. The peak of the wet season occurs in September and up to 530 mm falls in that month. The dry season is between the months December and April. The lagoon sits to the west of the coastal town of Puerto Escondido with 15°56'22.09"N and 15°55'35.93"N, and 97°9'21.24"W and 97°12'35.93"W as its boundaries, Figure 4. The lagoon is just over 5.5 km in length, and it is around 1 km wide. It has an average depth of around 5.4m, reaching a maximum depth of 15.0m (Torres-Ariño et al., 2020).

The lagoon is supplied with fresh water from the Manialtepec river that enters from the west. The river flows along a sandbank separating the river from the Pacific Ocean (Fig. 4B). In the sandbank there are two temporary connections with the ocean, located in Puerto Suelo and El Carnero (Contreras et al., 1997). These temporary connections are precipitation controlled and remain closed throughout most of the year. In the dry season, both connections remain closed. Then the lagoon is only supplied with fresh water from the river. At the height of the wet season both connections open and the last part of the river becomes saline, changing the composition of the supplied water into the lagoon. Empirical evidence from people who live around and work on the lagoon have spoken of two additional situations. In these situations either the opening in Puerto Suelo or El Carnero remain closed, whilst the other supplies the river with saline water. As a result of having four different phases of water supply, a strong salinity variance is present throughout the lagoon.

The land surrounding the lagoon has a wide variety of vegetation present. On the waterside a lot of red mangroves are found, which act as habitat for over 70 bird species, as well as various species of fish and other forms of coastal wildlife. The mangroves also maintain and protect the lagoon from wind

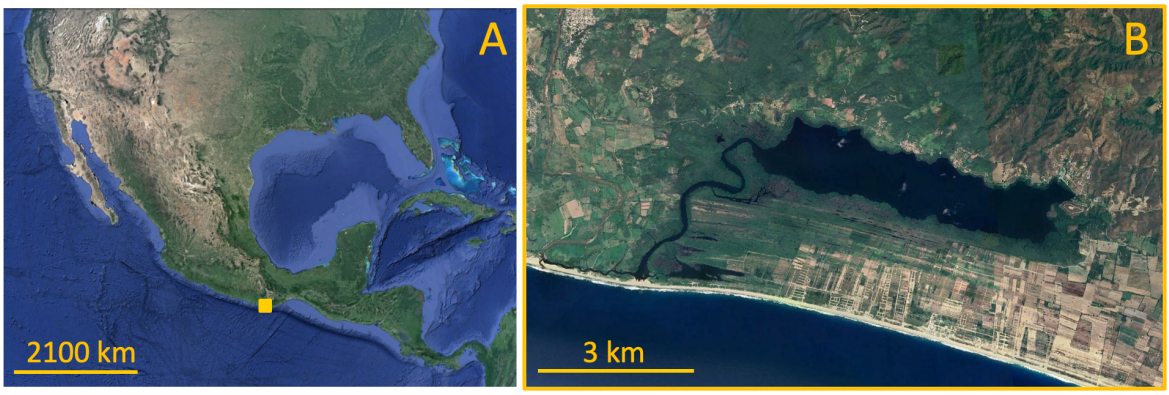

Figure 4: A. Map of North and Central America with location of the Manialtepec Lagoon (yellow square), B. zoomed in map of the Manialtepec Lagoon and its location in regards to the Pacific Ocean.

and water erosion. Other kinds of plants around the lagoon are aquatic and underwater vegetation, thorny shrubs, and coastal dune vegetation. Papaya cultivation and cattle ranching are the main types of agriculture present in the area, thus contributing anthropogenic influences.

A special inhabitant of the lagoon is a bioluminescent organism, commonly known as 'luminous plankton'. The luminous plankton can convert energy through chemical reactions, and as a result emit a blue light. This phenomenon is observed when it is dark, and preferably within a new moon phase so there is little to no light pollution (Arriola, 2021). Many tourists are attracted to the area to observe the luminescent phenomenon. Besides that the lagoon is also popular for bird and wildlife spotters. As a result, the lagoon has become very important for the local economy, with tourists supporting the small businesses that provide tours, food, and accommodation. Therefore, it is important for the lagoon to remain healthy for many years to come. By researching the carbon transport through the water we aim to understand the carbon fluxes through an estuary on a molecular scale better. However, the research could also shed light on to the conditions the 'luminous plankton' live in which would tell us more on why they produce light.

1.4 Research questions

In this work we investigate the the organic carbon distribution across the Manialtepec Lagoon in the state of Oaxaca, Mexico. From this lagoon samples were taken during a field work campaign at the end of October 2023. After which, biomarker analysis on FAs and GDGTs was performed at Utrecht University. By combining results from previous studies on bulk organic transport across estuaries and studies on biomarker analysis together with our analysis of the Manialtepec Lagoon we aim to obtain greater knowledge about the fate of organic matter in an estuary on a molecular scale. The main research question this paper focuses on is:

- How is organic matter transported across an estuary?

To answer the research question we study the following subquestions:

- What is the composition and distribution of FA and GDGT biomarkers in an estuary?
- What influence does the salinity gradient have on the organic matter?

2 Methods

2.1 Sample collection

The water and sediment samples used for this thesis were collected on a field campaign to the Manialtepec Lagoon in Mexico from 28 October to 31 October 2023. This was in between the wet and dry season they experience in southern Mexico, however no precipitation was recorded during the campaign. The campaign was facilitated by the Netherlands Earth System Science Center (NESSC). Five sampling locations were chosen on a trajectory from a starting point in the Manialtepec river (Hidalgo) to the far East side of the lagoon (Alejandria), as seen in Figure 5. These locations were predetermined by our collaborator Alejandra Torres Ariño, as she uses these sites for her own research to microbes in the lagoon. The locations were also in strategic locations for this project. Station Hidalgo is located in the river where there is only freshwater. At location Bocobarra Grande (7 km) there is one of the possible openings in the sand barrier. Here it is assumed that the saline water infiltrates the system by continuous seepage through the sand barrier. The Morrerias location (11 km) is at the start of the lagoon. This is the transition point where the system goes from more fluvial to coastal lagoon conditions. The last two locations, Isla del Gallo (15 km) and Alejandria (17 km) were chosen as they are representative of the lagoon at two different points. Together the five locations were expected to represent a clear transition from river to lagoon, including a clear salinity gradient.

Figure 5: Location of the Manialtepec Lagoon with the position of the five sampling sites (red arrows). Hidalgo is seen as the starting location (0 km) in the Manialtepec river and the four other locations have distances relative to Hidalgo indicated. For each site it is indicated what type of samples were taken there: surface water (Sur), bottom water (D), sediment (Sed), and soil (yellow circle).

From all locations surface water and sediment samples were taken. The surface water samples were taken from the boat using a plastic jug and filling a BPA free plastic water container. Each plastic water container was weighed to determine the total collected volume per sample. A small sediment grabber attached to a rope was used to collect the sediment samples. The sediment was transferred from the grabber to geological collection bags using a metal spoon.

At the locations Bocobarra Grande, Morrerias, and Isla del Gallo bottom water samples were also collected from just above the sediment layer. The respective depths were: 0.5, 1.5, and 5.5 m. The water was collected in the same BPA free plastic water containers, but instead of the jug a Niskin bottle was used to get the water from the side of the boat. All the collection and storage materials were rinsed in the surface water from each location three times before taking the samples.

From locations Hidalgo and Bocobarra Grande, and another point between them soil samples were taken from the river bank. A shovel cleaned with bottled water was used to collect soil from the upper centimeter at those locations. The samples were collected in geological bags.

Different physical parameters of the water samples were measured at each site. These were pH, oxygen concentration, and salinity. For this the plastic jug was filled with either surface or bottom water and taken on board the boat. The measurements were done with three probes: a Hach pHC101 probe, a Hach luminescenct dissolved oxygen probe, and a Hach conductivity probe. The probes were connected to a Hach HQd Portable Meter. Apart from the parameter the probe was intended for they each measured temperature, which were averaged to get the water temperature for each sample.

2.2 Core sampling

At 15°56.00'57"N and 97°12.00'7.00"W a sediment core was obtained during our sampling campaign. The core was taken in between the Morrerias and Isla del Gallo sampling locations, at around 13 km away from the starting point Hidalgo. This was done by throwing a modified hand core sediment sampler off the side of the boat, which was provided by Vladislav Carnero Bravo. The core sampler was fitted with an eggshell core catcher, which is needed to remove the core undisturbed from the sediment layer.

After this, the core sample was transported with utmost care back to the laboratories at the Universidad del Mar, Puerto Ángel. This was done to minimise disturbance to the layers and minimise inter-layer mixing. In the laboratory the core was sliced into sections of 1 cm and bagged individually in geological bags, with the help from students. During the slicing process a metal spatula was used to minimise organic material contamination.

The individual bags containing the core samples were all cold stored until their analysis at Utrecht University, the Netherlands. In this project only the top centimetre was used for GDGT analysis, and it was treated as another sediment sample in the trajectory.

2.3 Sample processing

Filtration of the surface and bottom waters was done using Whatman glass microfibre filters, Grade GF/F (0.7 μm). Using a tripod, Teflon tubing, and peristaltic pumps all water was passed through the filters which collected the suspended particulate matter (SPM). The filtrate was collected and about 40 mL of the filtrate was collected in a 50 mL vial for total DOC determination. Then the filtered water was acidified with concentrated HCl to pH 2, after which 0.5% (v/v) methanol was added. The acidified dilute was then passed through Agilent Bond Elut C18 Solid Phase Extraction (SPE) Cartridges (10 g bed, 60 mL) using cleaned tubing and peristaltic pumps. The SPE cartridges were pre-rinsed with 100 mL methanol and 50 mL acidified water (pH 2). The pumps were set to a sample flow of $\sim$40 mL/min once the tubing was connected to the samples. After the entire sample was filtered the cartridge was rinsed with 50 mL acidified water. The filters, SPE cartridges, and sediments were all cold-stored until their analysis at Utrecht University, the Netherlands.

Additionally, three soil samples were taken from the main sandbank, a mangrove bank, and along the river. Filters, sediments, and soils were all freeze dried back in Utrecht, and a $<$63 μm size fraction was made of the sediments and soils before further analysis.

2.4 Total DOC concentration determination

Dissolved Organic Carbon (DOC) was measured on a Shimadzu TOC-V CP analyser. The analysis is done using an infrared (IR) detector that detects water vapour and CO_2. The TOC-V CP cannot directly measure DOC in water samples, but rather total carbon (TC) and total inorganic carbon (TIC). TIC was measured by passing the sample through phosphoric acid where IC (e.g. carbonate, bicarbonate) is released as CO_2. This passes the IR detector and TIC is determined. During the TC measurement the sample water passes an oven containing a platinum grain catalyst. Here all carbon

oxidises to CO_2, which is measured by the IR detector. By subtracting TIC from TC a value for DOC in the water is obtained.

2.5 DOC extraction from cartridge

The SPE cartridges were brought to room temperature before DOC extraction. At room temperature the cartridges were washed with 80 mL methanol using gravity. The elute was collected in two 60 mL collection vials per cartridge. The methanol was dried under N_2 gas at 40 °C. The total lipid extracts (TLEs) were transferred to 4 mL vials using methanol and dried under N_2 gas at 40°C.

2.6 Microwave extraction of POC

The sediments, soils, and filters were extracted in 25 mL dichloromethane (DCM):methanol (9:1) with the Milestone Ethos X (MEX) microwave-assisted extraction system. For sediments and soils, between 0.98 and 3.24 g of sieved <63 μm size fraction was extracted per sample. The weight depended on the expected carbon content of the individual samples. Around 80% of the dried filters were extracted, the rest of the filters was stored for elemental analysis. After the MEX program the solvent was decanted into 60 mL collection vials and the samples were washed twice with 10 mL DCM:methanol (9:1). The solvent was dried under N_2 gas before the TLE was filtered over a sodium sulphate column and collected in a 4 mL vial.

2.7 Lipid biomarker analysis in DOC and POC

The TLEs received an acid hydrolysis treatment by adding 0.5 mL of HCl in methanol (1.5N) to a sample vial. Then, the vials were placed in an oven at 70°C for two hours with a closed lid. After two hours the samples were cooled to room temperature and 0.5 mL MilliQ water and 1 mL DCM was added. The vials were vortexed, and the bottom layer (DCM-layer) was decanted off with a pipet. The vials were washed twice more with 1 mL DCM and the DCM was dried under N_2.

Next, 0.5 mL DCM:methanol (1:1) was added to the sample vials. Then the vials were transferred to a fume hood for the methylation of the TLE. Here, 10 μL TMS-diazomethane (2M) was added to each vial and was left to react for a few minutes with the lid open, and then 30 minutes with the lid closed. After 30 minutes the reactions were stopped by adding 10 μL acetic acid (2M) and the vials were immediately dried under N_2. The samples were dissolved in a total of 3 mL ethyl acetate and eluted over a deactivated silica gel column with a small layer of sodium carbonate on top.

The prepared lipid extracts were then separated into three fractions: an apolar, a neutral, and a polar fraction. To achieve this the lipids were eluted over an aluminium oxide column with three different solvents: hexane:DCM (9:1), hexane:DCM (1:1), and DCM:methanol (1:1), respectively.

Neutral fraction analysis, for fatty acid detection, was performed on a Hewlett Packard 6890 series gas chromatogram coupled to a flame ionization detector (GC-FID). The neutral fractions were dissolved in a known amount of hexane of which 1 μL was injected into the GC-FID along with 1 μL squalene (63.8 ng/mL) as external standard. Using helium gas as carrier the sample passed through an Agilent VF-1ms non-polar column (Length: 30 m, Inner Diameter: 0.32 mm, Film Thickness: 0.10 μm) at a constant pressure of 100 kPa. The oven temperature increased from 70°C to 130°C at 20°C per minute, after which it increased to 320°C at 4°C per minute, where the temperature remained constant for 10 minutes.

To identify the peaks obtained on the GC-FID an Agilent 7890B series GC equipped with a CP-Sil 5 CB column (length: 25m, diameter: 0.32 mm, film thickness: 0.12 μm) coupled to an Agilent 5977B MSD mass spectrometer (GC-MS) was used. The oven settings on the GC-MS were the same as for the GC-FID and it operated under a constant N_2 gas flow of 1.6 mL per minute and the MS worked between 50 – 800 m/z as scanning range.

Using an Agilent 1260 Infinity High Performance Liquid Chromatography-Mass Spectrometer (HPLC-MS) the polar fraction was analysed for the presence of GDGTs (Hopmans et al., 2016). The method by

Hopmans et al., 2016 was developed specifically for GDGT analysis. The sample preparation consisted firstly of adding 1 mL C_{46}-GDGT internal standard (152 ng/mL) to the vials. Then, dissolving the vial contents in a predetermined amount of hexane:isopropanol (IPA) (99:1) and filtering it over a 0.45 μm polytetrafluorethylene filter. Through auto-injection 10 μL sample was injected, after which the compounds were separated over two Waters UHPLC BEH Hilic columns (1.7 μm, 2.1 mm x 150 mm) with a flow rate of 0.2 mL per minute. At a constant temperature of 30°C the polar fraction was eluted for 25 minutes using 82% hexane and 18% hexane:IPA (9:1. After which the mobile phase changed linearly to a composition of 70% hexane and 30% hexane:IPA (9:1) in 25 minutes.

After separation the compounds were ionized by atmospheric pressure chemical ionization. For this, the gas temperature was set at 200°C, vaporizer temperature 400°C, the N_2 gas flow at 6 L per minute, capillary voltage at 3500 V, nebulizer pressure at 25 psi, and the corona current at 5.0 μA. GDGT detection was done by single ion monitoring (SIM) of the positive ions and quantified using the integration function on Chemstation B.04.03 software. The $[M\text{-}H]^+$ ions that were used were: m/z 1018, 1020, 1022, 1032, 1034, 1036, 1046, 1048, 1050, 1292. The C_{46} GDGT internal standard was identified with m/z 744.

2.8 Stable carbon isotope analysis of POC

From the remaining 20% of the dried filters a punch with a diameter of 5 or 8 mm was taken to determine stable isotope ($^{13}C/^{12}C$) ratios of the POC. The punches were fumigated for 20 hours in a desiccator containing a Petri dish with fuming HCl (37%). After fumigation the punches were dried in an oven at 60°C for over five hours. The punches were folded into a tin capsule and then placed in the auto-sampler of a ThermoFisher Scientific Elemental Analyser Isotope Ratio Mass Spectrometer (EA-IRMS), along with nicotinamide and granite quartz (GQ) as standards. The samples were oxidized in a Flash IRMS EA where all carbon reacts to CO_2 in an oven at 1020°C, with helium acting as carrier gas. Regulated by the CONFLO IV universal interface the CO_2 is injected to Delta V Advantage IRMS where the isotope ratios are determined. The isotope ratios were reported in the $\delta^{13}C$ notation against the Vienna Pee Dee Belemnite (V-PDB) standard. The obtained values for total carbon percentages and $\delta^{13}C_{V-PDB}$ vary with 5.4% and 0.08‰ respectively, based on the analytical error calculated from the nicotinamide standard.

3 Results

3.1 Physical parameters in the Manialtepec Lagoon

The salinity in the surface waters increased from 0.08‰ to 7.88‰ at 17 km at the time of sampling in October 2023. The pH increased from 7.5 to 8.2 along the trajectory. A similar increase was measured for the oxygen concentration going from 7.37 mg/l to 8.51 mg/L travelling into the lagoon (Tab. 1). Up until the mouth of the lagoon the surface water temperature was measured between 29-30°C, but after the mouth of the lagoon (from 11 km) the surface water temperature was measured between 32-34°C. The parameter results are plotted in Figure 6 at the corresponding sampling sites.

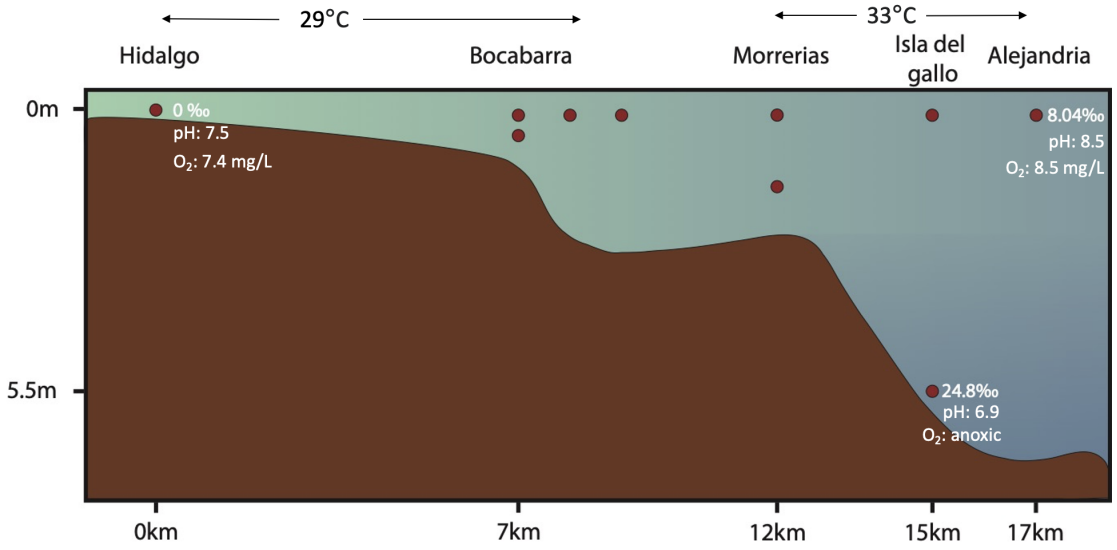

Figure 6: A cross section of the trajectory of the Manialtepec lagoon. The sampling locations are positioned at the distance they are removed from Hidalgo (red dots). There are two additional points between Bocobarra and Morrerias which is where the same parameters were measured by Alejandra Torres Ariño for her own research. These results were incorporated to create a longer salinity gradient. The pH, O_2, and salinity results were plotted at Hidalgo, Isla del Gallo (bottom water), and Alejandria.

At depth, the salinity increased slightly between 5 and 11 km from 4.15‰ to 7.99‰, afterwhich it increased drastically to 24.8‰ at 15 km and showed higher values than the surface waters. The salinties at the surface were 1.52, 6.62, and 7.85‰ respectively. The pH levels went from 6.91 to 7.83 and then back down to 7.26. All of which were lower than the respective surface waters. The oxygen concentration at 7 km was 6.53 mg/L, but the other locations had no measurable oxygen levels. The anoxia in the bottom waters was also confirmed by the strong sulphuric smell that came from the water. At 7 km the temperature was 28.6°C, and the two locations in the lagoon were 32.6°C and 32.1°C respectively.

Table 1: Salinity, oxygen concentration (mg/L), pH, and temperature (°C) of the surface and bottom water samples of the Manialtepec Lagoon between 28 - 31 October 2023.

Location	Distance (km)	Salinity (‰)	O_2 (mg/L)	pH	T(°C)
Hidalgo	0	0.08	7.37	7.52	29.9
Bocabarra	7	1.52	6.48	7.47	29.5
Morrerias	11	6.62	-	8.17	32.2
Isla del Gallo	15	7.85	8.11	8.16	34
Alejandria	17	8.51	7.88	8.19	33.8
Bocabarra (bottom)	7	4.15	6.53	7.26	28.6
Morrerias (bottom)	11	7.99	-	7.83	32.6
Isla del Gallo (bottom)	15	24.8	-	6.91	32.1

3.2 Concentration and isotopic composition of bulk organic carbon

In the surface water the bulk DOC concentration increases with an increasing salinity, Table 2. At 0 km the DOC concentration was 4.10 mg/L which increased to 11.47 mg/L at the sampling location with the highest surface water salinity. The bottom waters showed a different pattern where the DOC concentration increased from 4.87 mg/L at 7 km to 11.29 mg/L at 11 km, only for it to decrease at 15 km to 9.14 mg/L. Going from 7 km to 11 km was the part of the trajectory where the salinity increased the most, and from 11 km to 15 km was the section going from the start of the lagoon to over half way down the lagoon.

Table 2: Concentrations (mg/L) of bulk dissolved organic carbon (DOC) and particulate organic carbon (POC) in the surface and bottom water samples of the Manialtepec Lagoon between 28 - 31 October 2023. Also, stable carbon isotope ratios of POC in surface and bottom waters of the Manialtepec Lagoon reported in the $\delta^{13}C_{V-PDB}$ notation.

Location	Distance (km)	DOC (mg/L)	POC (mg/L)	δ^{13}C (‰)
Hidalgo	0	4.10	0.03	-26.7
Bocabarra	7	4.97	0.13	-29.7
Morrerias	11	10.66	0.97	-30.7
Isla del Gallo	15	11.43	1.62	-30.0
Alejandria	17	11.47	1.50	-30.4
Bocabarra (bottom)	7	4.87	0.07	-30.4
Morrerias (bottom)	11	11.29	1.71	-30.1
Isla del Gallo (bottom)	15	9.14	0.10	-29.2

From the stable carbon isotope analysis the bulk POC concentrations were able to be calculated, Table 2. The POC concentrations showed a similar trend in the surface waters as the DOC where concentrations increase over the trajectory. Going from 0.03 mg/L in fresh water at 0 km to 1.62 mg/L in saline waters at 15 km. The bulk POC concentration in the surface water at 17 km is a bit lower at 1.50 mg/L. The bottom waters showed the same pattern as in the DOC where the concentration increases from Bocabarra to Morrerias, this is also where the largest salinity increase occurs, only for it to decrease again to Isla del Gallo.

From the stable carbon isotope analysis the $\delta^{13}C$ signatures were also obtained, Table 2. In both surface and bottom waters the samples were depleted in ^{13}C with values ranging from -30.7‰ to -29.2‰. However, one sample stood out in $\delta^{13}C$ value, namely the sample taken at 0 km with a less negative value of -26.7‰, being a lot less depleted in ^{13}C compared to the other samples. This sample was taken from the river (fresh water), whereas the other samples came from locations with higher salinity concentrations (Tab. 1).

3.3 Fatty acid composition and distribution across the lagoon

Total concentrations of FAs in the DOC, SPM, and sediment fraction were calculated by combining the concentration of each detected FA per fraction for each sample. In the total FA concentrations, there is a decreasing trend in FAs in the surface water DOC travelling further into the lagoon, as seen in Figure 7A. The total FA concentration in the DOC of surface waters decreases from 1.95 to 0.69 mg/g_C going from 0 to 7 km in the trajectory. After 7 km there is a slight increase in total FA to 0.90 mg/g_C at 11 km. This section is where the salinity increases the most and the system changes from fluvial to lagoonal. The concentration then decreases to 0.50 mg/g_C towards the far end of the lagoon (17 km), Figure 7B. Total FAs in the DOC of bottom waters decrease in concentration at the intersection of a fluvial and lagoonal system from 3.20 to 0.74 mg/g_C, after which the concentration increases to 3.78 mg/g_C at Isla del Gallo (15 km).

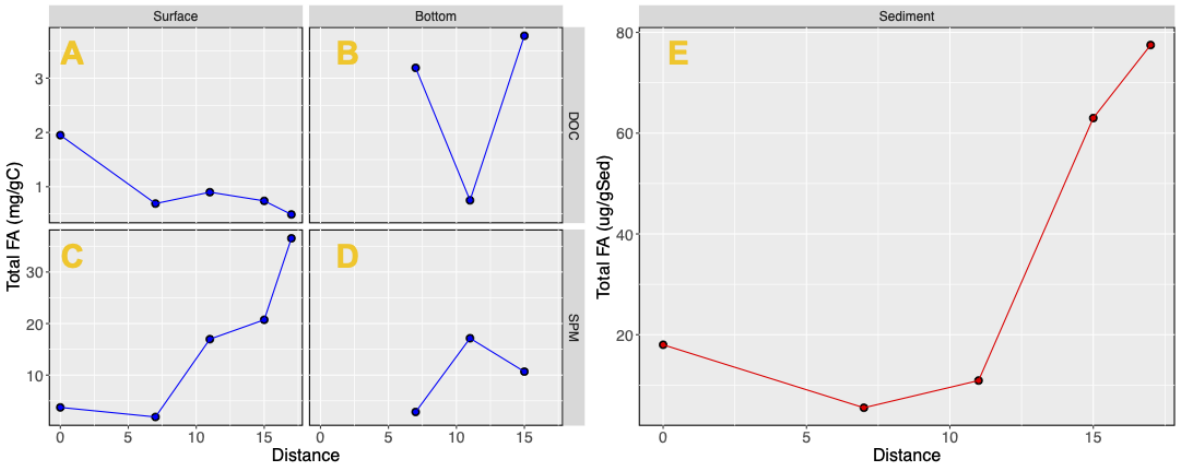

Figure 7: Total concentration FAs measured in surface and bottom waters (mg/g_C) for both DOC (A and B) and POC (C and D) fractions, and total concentrations FAs measured in sediments ($\mu g/g_{sediment}$) (E) plotted against distance in km, going from fresh (0 km) to saline waters (17 km).

In the DOC only a few saturated FAs (SFAs) were detected, namely saturated $C_{14:0,16:0,18:0}$, and also some unsaturated FAs $C_{16:1,18:2}$ which can be attributed to phytoplankton and some bacterial communities. The concentrations of individual FAs in the DOC are depicted in Figure 8A. Most FAs in the DOC decreased in concentration from 0 km to 7 km in the surface waters. The concentrations at the mouth of the lagoon were higher for C_{16} and C_{18}, after which they decreased again towards the far sampling point in the lagoon. The bottom waters showed a strong decrease in FA concentrations from 7 km to 11 km, only for the concentrations to increase more going to 15 km. C_{16} showed the largest variation in the bottom waters going from 1.89 mg/g_C to 0.43 mg/g_C, to then increase up to 1.57 mg/g_C.

The total concentration of FAs in SPM showed an inverse trend compared to the DOC, Figure 7C. In the surface waters the concentrations of saturated and unsaturated FAs increased along the trajectory from 3.73 mg/g_C at 0 km to 36.63 mg/g_C at 17 km. The same inverse trend compared to the DOC fraction was seen in the bottom waters, Figure 7D. In the SPM the total concentrations of the FAs increased at the section where the system changed from fluvial to lagoonal from 2.84 mg/g_C to 17.17 mg/g_C. Only for it to decrease again to 10.66 mg/g_C going further into the lagoon (15 km).

A wider variation of FAs were observed in the SPM fraction compared to the DOC fraction, which can be found in Figure 8B. The additional FAs in the SPM were saturated $C_{15:0,20:0,22:0}$ and unsaturated $C_{18:1,20:5,22:1}$ FAs, these are often attributed to microbial production. In surface waters ΣSFA increased from 0.7 mg/g_C to 21.9 mg/g_C, and in bottom waters they increased from 1.3 mg/g_C to 10.0 mg/g_C after they decreased to 6.7 mg/g_C. The ΣSFAs showed similar trends in surface and bottom waters, but with slightly lower concentrations. However, some FAs in the SPM do not increase along the

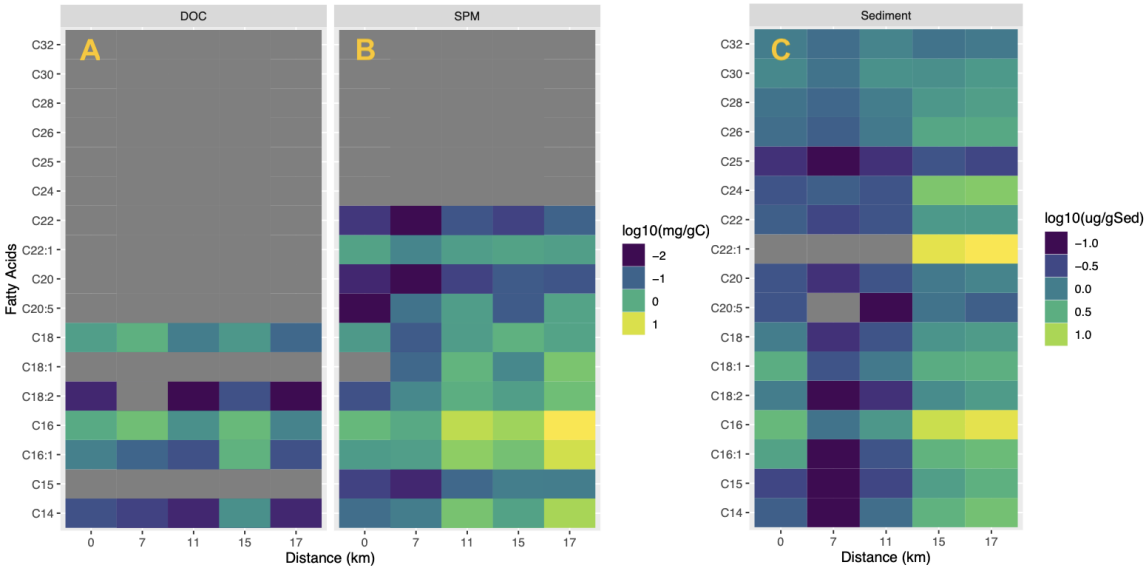

Figure 8: Heatmap of concentrations of all detected FAs in DOC (A) and SPM (B) (log10(mg/g_C)) on the left and concentrations of all detected FAs in sediments (C) (log10(μg/g Sed) on the right plotted individually against distance in km, going from fresh (0 km) to saline waters (17 km).

trajectory. $C_{18:0,20:0,22:0,22:1}$ show stable concentrations throughout the trajectory. The other FAs contribute to the increase of total FAs in the SPM.

The total FA concentrations in the surface sediment samples show a strong increase across the entire trajectory, showed in Figure 7E. Initially the concentration decreases from 18.16 $\mu g/g_{sediment}$ to 5.54 $\mu g/g_{sediment}$ in the fluvial part of the system. At the transition point from 5 to 7 km a small increase to 10.82 $\mu g/g_{sediment}$ is observed. From there the concentration increases strongly to a maximum of 77.59 $\mu g/g_{sediment}$ at the Alejandria station.

The sediment samples showed the widest variation in types of detected FAs, with middle chain (C_{22}-C_{26}) and long chain FAs ($>C_{28}$) also being present, as well as all the other FAs detected in the DOC and SPM. The ΣSCFAs ($<C_{20}$) increases from 2.3 $\mu g/g_{sediment}$ at 5 km in the fluvial section of the system to 63.1 $\mu g/g_{sediment}$ at the last location in the lagoon. For the medium and long chain FAs an increase is also observed after 11 km, however not so large as the SCFAs, increasing from 3.1 $\mu g/g_{sediment}$ to 14.1 $\mu g/g_{sediment}$. The two most dominant short chain FAs were $C_{16:0}$ and C_{22} having maximum concentrations at 17 km of 22.8 $\mu g/g_{sediment}$ and 28.4 $\mu g/g_{sediment}$ respectively. The long chain FAs were not as abundant with C_{24} showing a maximum concentration of 8.3 $\mu g/g_{sediment}$.

Using the Average Chain Length (ACL) index of the FAs a clear distinction can be made between the FA distribution of the DOC, SPM, and sediments. For both surface and bottom waters, the ACL is constant along the transect in each water fraction. Namely, around 16.5 in DOC and 21.1 in SPM. The sediments however showed higher ACL values than DOC and SPM. The sediments also showed a higher ACL in the lagoon, compared to the river. In the river section the sediments had an ACL of 25.4, and in the lagoon, it increased to 27.5.

3.4 GDGT composition and distribution across the lagoon

The total concentration of brGDGTs and isoGDGTs were calculated by taking the sum of all individually measured GDGTs (Fig. 9). In the surface waters both the total brGDGTs and isoGDGTs show a strong decrease in concentration along the trajectory of the lagoon. The isoGDGTs decreased from 27.95 $\mu g/mg_C$ at 0 km to 0.73 $\mu g/mg_C$ at 11 km, and eventually dropping to 0.15 $\mu g/mg_C$ at 17 km. The brGDGTs showed a similar pattern but decreasing from 59.39 $\mu g/mg_C$ to 1.03 $\mu g/mg_C$ at 11 km, to 0.16 at the last sampling location.

Both the brGDGTs and isoGDGTs had concentrations that decreased between 7 km and 11 km in the bottom waters, only for them to raise again going towards 15 km. The main difference in the deep-water samples was that in the isoGDGTs the decrease was smaller than the increase in concentration, whereas for the brGDGTs, that was the other way around.

Total concentrations showed the most variation in the sediment samples. The sediment results also contain data that was obtained from the core mentioned in Section 2.2. Of the core, the first centimetre was used as a sediment sample. Initially, the concentration decreased in both brGDGTs and isoGDGTs from the sampling site at 0 km to the site at 11 km. After which, in both cases a strong increase of concentration occurred towards the sample at 13 km. Following the strong increase, both GDGTs decreased towards 15 km, and ended in an increase towards 17 km. The concentration range of the total brGDGTs in the sediments was from 115.73 $ng/g_{sediment}$ to 732.03 $ng/g_{sediment}$. A broader range was observed for the isoGDGTs where the concentrations varied from 64.12 $ng/g_{sediment}$ to 1627.72 $ng/g_{sediment}$.

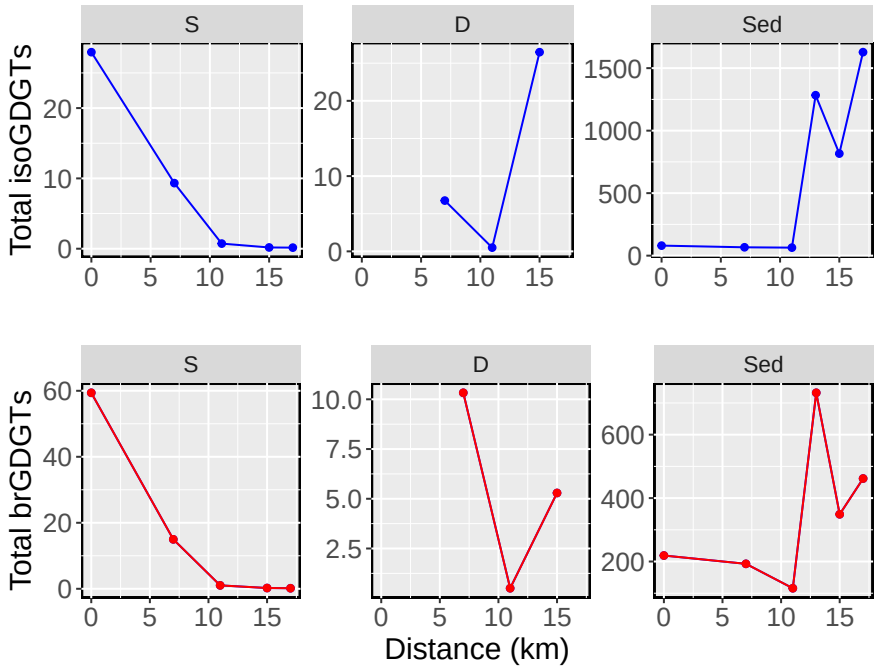

Figure 9: Concentrations of total isoGDGTs (blue lines) and total brGDGTs (red lines) in surface (S) and bottom water (D) ($\mu g/mg_C$) and sediments (Sed) ($ng/g_{sediment}$) plotted against distance in km, going from fresh to saline water.

Analysing the plotted concentration of each GDGT in a heat- (Fig. 10), it became apparent which GDGTs were dominant in the system. In the surface water, the main brGDGT detected was Ia. At 0 km IIa' was also present in higher concentration than others. In the sediments Ia was also the most abundant brGDGT. For the isoGDGTs, GDGT-0 was the most abundant in surface and bottom waters and sediments. Crenarchaeol was the second most dominant isoGDGT across the system.

It can also be observed that across sediments, surface waters, and bottom waters the GDGT distribu-

tion remained almost the same for each type of sample and location of where the sample was taken. This is not the same as the FAs, where each type of sample had its own fingerprint of what FAs were present.

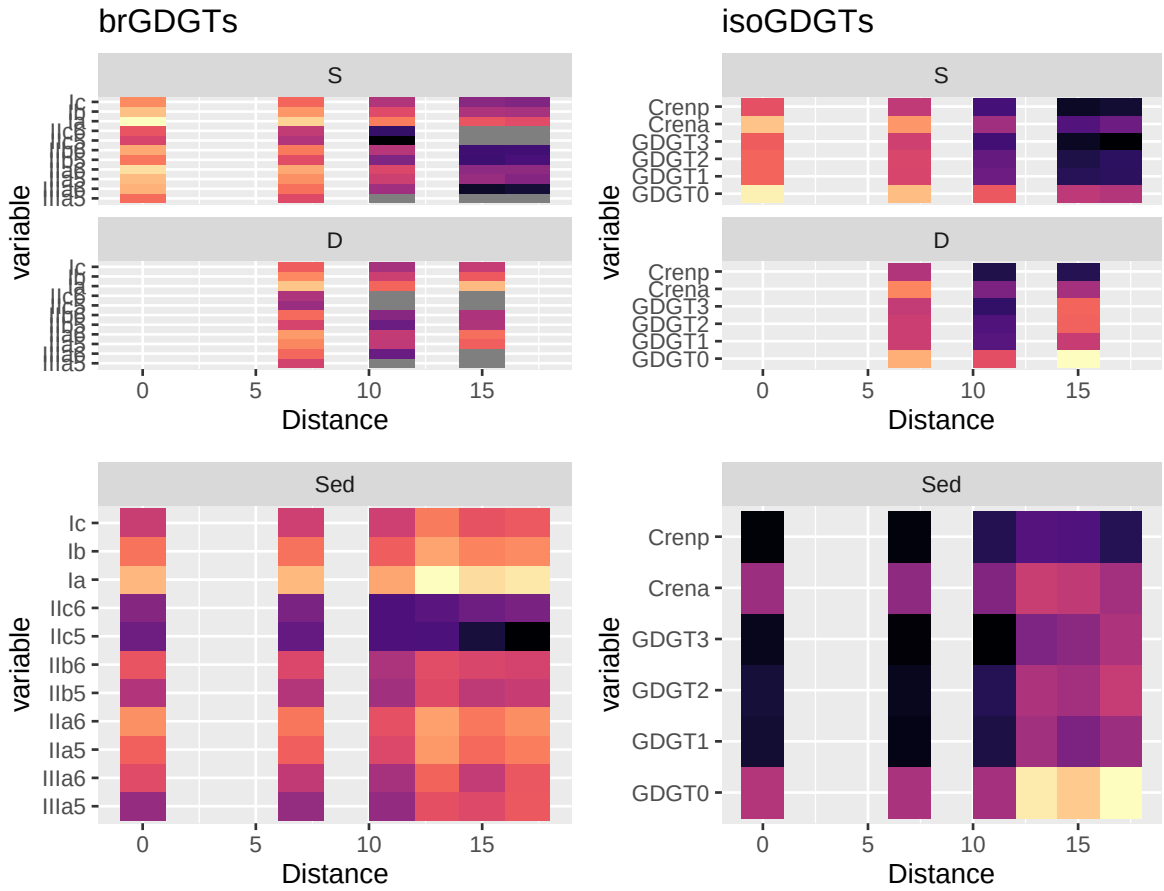

Figure 10: Heatmap of concentrations of all detected GDGTs plotted individually against distance in km, going from fresh to saline waters. On the left are all brGDGTs found in surface (S) and bottom (D) waters and sediments (Sed) and on the right all isoGDGTs found in the same phases (S, D, and Sed).

Using the relative abundances of the brGDGTs and isoGDGTs (Fig. 10) BIT values were calculated using Equation 10. The values ranged between 0.66 and 0.98 with an average of 0.89, and can be found in Table 3.

Table 3: Table containing the calculated BIT values, using Eq. 10, for the surface and bottom water and the sediment samples taken from the Manialtepec lagoon.

Location	Distance (km)	BIT (surface)	BIT (depth)	BIT (sediment)
Hidalgo	0	0.88	-	0.66
Bocabarra	7	0.83	0.98	0.67
Morrerias	11	0.92	0.93	0.68
Isla del Gallo	15	0.95	0.93	0.83
Alejandria	17	0.88	-	0.88

Additionally, the Methanogenesis GDGT-0/crenarchaeol ratio was determined using Equation 3 to analyse the methanogenic input on the samples. Values ranging from 1.5 to 45.8 were obtained across the trajectory. In the deep water sample from the Isla del Gallo location a substantial outlying value was calculated of 293.5. The Methanogenesis values can be found in Table 4.

Table 4: Table containing [GDGT-0]/crenarchaeol ratios, using Eq. 3, for the surface and bottom water and the sediment samples taken from the Manialtepec lagoon.

Location	Distance (km)	$\frac{[GDGT\text{-}0]}{[cren]}$ (surface)	$\frac{[GDGT\text{-}0]}{[cren]}$ (depth)	$\frac{[GDGT\text{-}0]}{[cren]}$ (sediment)
Hidalgo	0	2.7	-	1.5
Bocabarra	7	2.4	2.5	1.6
Morrerias	11	8.	15.0	1.9
Isla del Gallo	15	15.7	293.5	12.9
Alejandria	17	6.2	-	45.8

4 Discussion

4.1 Distribution of biomarkers in Manialtepec Lagoon

4.1.1 Spatial variation in fatty acid distribution across the river-lagoon transect

When observing the trends of the FAs across the trajectory across the lagoon it becomes clear that as the salinity increases going into the lagoon. The concentration of total FAs in the surface water SPM fraction and in the sediments increase from 0 to 17 km. This increase occurs along the entire trajectory, but it is highest between the sampling locations at 7 km and 11 km (Fig. 7A and E), which is also the point where the salinity shows the largest increase (Tab. 1). At this interface between fresh and salt water the ecological niches change causing FAs to produce in the water column.

In the lagoonal section the largest concentration increases are of $C_{16:0}$, $C_{16:1}$, $C_{22:1}$, and $C_{24:0}$. $C_{16:0}$ and $C_{16:1}$ are both produced by phytoplankton communities and can indicate the presence of cyanobacteria. The MUFA $C_{22:1}$ is produced planktonally, and $C_{24:0}$ is often found on terrestrial plant waxes, but can also be produced microbial. The increase of the along the trajectory is most likely caused by in situ microbial primary production.

In the Manialtepec system the concentrations of $C_{20:5}$ are very low, all remaining under 1.0 mg/g_C in SPM and 1 $\mu g/mg_C$, and remaining stable across the trajectory. The presence of $C_{20:5}$ does however indicate algal input into the system (W. Guo et al., 2019). The low concentration of $C_{20:5}$ does not necessarily indicate little algal primary production, as there are other FAs that are produced algally(Derrien et al., 2017). However, these other FAs are produced ubiquitously in the environment and cannot be used as biomarkers. Additionally, bacterial production in the water column can degrade algally produced acids, as they are more labile due to the double bonds. There are many other lipid biomarkers that indicate algal production (e.g. certain sterols and n-alkanes). By analysing them, algal production in the Manialtepec lagoon could be better understood. Further research is required to determine the algal presence in the lagoon.

In the DOC fraction of surface and bottom waters opposing trends of FA concentration can be observed, compared to the trends in SPM (Fig. 7C). In the surface water DOC a decreasing trend in total FA concentrations is observed with an increasing salinity. In the bottom waters the FA concentration increase at the mouth of the lagoon, after which they decrease again further into the lagoon. The removal of FAs from the DOC fraction can be attributed to flocculation, remineralisation, but also to microbial uptake in the water (Carlson et al., 2010). The microbial uptake of DOC can be explained by the clear increase of FAs in SPM. It is thought that microbial primary production consumes algally produced acids from the water.

Red mangroves (Rhizophora Mangle) are the main type of terrestrial vegetation around the lagoon (Arriola, 2021). Terrestrial higher plant biomarker lipids are indicated by long chain saturated FAs (Matsuda & Koyama, 1977). In our samples they are only present in the sediment layer, with higher concentrations in the the fluvial, fresh water section of the system (0 to 11 km). Mangroves being terrestrial higher plants will produce $C_{24:0}$, $C_{26:0}$, $C_{28:0}$ FAs (Resmi et al., 2023).

There could be a variety of reasons for the lack of long chain FAs in the DOC and SPM fractions. Chemical interactions in the water column, such as microbial degradation, oxic-anoxic oscillations, and bioturbation in the river are possible sinks of long chain FAs (Middelburg & Herman, 2007). Another reason could be the time frame the samples cover. The water samples are effectively a snapshot of the exact time the samples were taken, whereas the sediment samples cover a larger integration time. As the long chain FAs often come from plant leaf waxes, they are usually washed off by precipitation. As our samples were taken in a period with no precipitation, it is possible that these leaf waxes were not even present in the water column as there was no water runoff entering the fluvial system. The sediment layer is built up over a longer period of time and likely also covers the parts of the year with precipitation where the surface runoff (including the plant leaf waxes) enter the water. Therefore, it could be possible for the long chain FAs to be observable in the sediment and not the water column. Thus, this observation is not necessarily caused by chemical interactions.

Using the ACL (Eq. 1) index for FAs, a prediction can be made about the relative input of terrestrial or marine FAs in the system. The DOC phase has an ACL of 16.5 and the SPM has a value of 21.1. Higher ACL values are found in the sediment layer. Where the fluvial section had an ACL value of 25.4, the the lagoonal section had a value of 27.5. As values $\leq$ 18.6 indicate dominant marine input, it is thought that the DOC has high marine activity. The sediments show strong terrestrial input with values $\geq$ 23.3. As the ACL value of SPM is 21.1, a mixed input of marine and terrestrial OM is present for this phase.

Leaf litter is the most prominent source of OM in mangroves. The long chain saturated FAs measured in the sediment layer most likely originate from this leaf litter. The δ^{13}C values from the bulk OC data can be used to specify this assumption (Yoneyama et al., 2010). In the lagoon, an average δ^{13}C value of -30.1‰ was measured. This falls within the δ^{13}C range for C_3 plants, which is -31.6‰ to -25.2‰. Mangroves usually have δ^{13}C of around -27‰, as they are C_3 plants (Bouillon et al., 2008). For this reason, the lagoonal sediments contain different sources of OC giving values more depleted in ^{13}C. The river section has a δ^{13}C of -26.7‰ which is closer to that of mangroves.

The lack of variation of FAs in the DOC and SPM phases can be attributed to high level of reworking and recycling of algal and potentially terrestrial fatty acids. As a result, total FA concentration increases across the trajectory. Furthermore, the increase of total FAs could be a result of accumulation of SPM at the far end of the lagoon, as there is no way for the water to exit the system at this end. This argument is however dismissed by the fact that certain individual FA concentrations, of for example $C_{15:0}$ and $C_{20:0}$, do not increase into the lagoon. If accumulation was the cause of high concentrations at the end of the lagoon, all FAs would increase along the transect. Due to the potential high reworking of the long chain FAs in the river, it can be said that the even $>C_{24:0}$ FAs are transported from close by to the sediments. As a result of reduced water velocity in the lagoon and the topography of the sediment layer causing close-by transportation.

4.1.2 Spatial variation in isoGDGT and brGDGT distribution across the river-lagoon transect

As mentioned before, the fractional distribution of the FAs shows differences between the samples from surface waters, bottom waters, and sediments (Fig. 8). More types of FAs were detected in the sediment layer, and varying trends of individual FAs were observed across the transect. Some FAs increased in concentration from the river to the far end of the lagoon, whereas other FAs remained steady in concentration across the trajectory. Each FA had its own chemical signature across the lagoon.

With the measured GDGT concentration different trends in fractional distributions were observed compared to the FAs (Fig. 10). In all samples GDGT-0 to GDGT-3, as well as crenarcaeol and its isomer were measured as isoGDGTs. For the brGDGTs, all variations of I and II were observed, but for the hexa-methylated brGDGT the molecules with no cyclopentane moieties were measured (IIIa & IIIa'). The fractional abundances of the detected GDGTs remained the same across each sample. The total brGDGTs and isoGDGTs concentration decreased going along the trajectory into the lagoon. The opposite was observed in the sediment layer where brGDGTs and isoGDGT concentrations increased from the river to the far end of the lagoon (Fig. 9). The bottom waters showed a decrease in GDGTs at the fresh-saline water interface, after which the concentrations increased again going further into the lagoon. Where the FAs had an individual chemical signature, the GDGTs showed a fractional chemical signature that remains the same for each GDGT in the surface water, bottom water, or sediment layer.

From the GDGT concentration obtained from our samples, TEX_{86} values were calculated. They ranged from 0.60 to 0.89 with an average of 0.71. No strong correlation was found between the location of the sample and TEX values, both across the estuary, and through the water column and sediments. High average SSTs are associated with the high TEX values obtained in the Manialtepec samples, which comes to no surprise as the lagoon is situated in the tropics. Also, the measured air and water temperatures at the Manialtepec lagoon are in the upper region of the SST calibration from TEX_{86}. At these temperatures the calibration error is large, making the calculated SSTs less accurate (Tierney & Tingley, 2014). Additionally, isoGDGTs with zero to three cyclopentane moieties have been shown to be produced by methanogenic archaea in lacustrine water columns and in sediments. As these methanogenic isoGDGTs are prominent in the TEX_{86} equation (2), a large overprint of methanogens can occur in lacustrine samples (Blaga et al., 2009). This results in a less accurate and reliable TEX_{86} proxy in lacustrine environments.

As seen in Table 3 (Section 3.4), the calculated BIT values ranged from 0.61 to 0.98 with an average of 0.89 in the Manialtepec samples. Also here, no clear trend was observed between the sampling locations across the transect, and the corresponding BIT values. The high BIT values (>0.60) do indicate a large terrestrial input for the GDGTs in the system. This is however not surprising, as the Manialtepec lagoon is separated from the open ocean most of the year. Lakes usually tend to have a higher measured terrestrial input due to soil erosion caused by precipitation (eg. Blaga et al., 2009, Damsté et al., 2009, Tierney et al., 2010). Additionally, the CBT'_{5Me} and MBT'_{5Me} values were not considered in this project, as tetramethylated brGDGTs were so dominantly present in the system. As a result, no significant changes in CBT'_{5Me} and MBT'_{5Me} values across the estuary were observed.

Considering the limitations of using the TEX_{86} and BIT proxies in warm and lacustrine environments, as well as there being no observable trends in values across the estuary, a different approach was used for the GDGT data analysis. For this, a principal component analysis (PCA) was performed to see if a clear variation in GDGT distrubution can be found between the different types of samples. To perform a PCA, the fractional abundances of all detected GDGTs, in all samples, were plotted against each other, as seen in Figure 11.

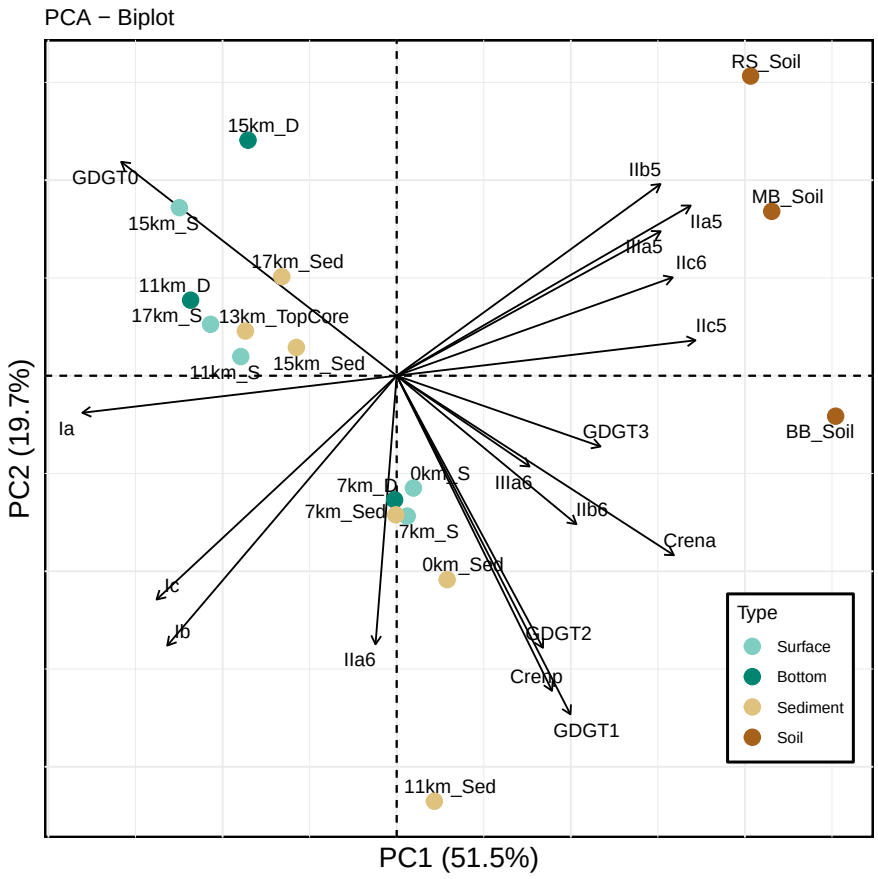

Figure 11: Principle component analysis of fractional abundances of all brGDGTs and isoGDGTs measured in the Manialtepec lagoon samples.

From the PCA it becomes clear there are three main clusters of samples with similar GDGT compositions. The first cluster contains the soil samples and can be found mostly in Quadrant I. The GDGTs that are associated with these samples are IIa, IIb, IIc, IIC' and IIIa. The cluster of soil samples consists of three samples taken from the bank of the Manialtepec river before the river had reached the lagoon. River bank (RS_Soil), mangrove bank (MB_Soil), and sandbank (BB_Soil) are the locations of where the soils where taken from. The soil samples plot in their own cluster seperated from where the surface and bottom water and sediment samples plot, indicating their own signature GDGT composition.

The second cluster is found in Quadrant II and contains lagoonal samples. The lagoonal cluster samples are dominated by GDGT-0. The sampling locations of this cluster are all in the lagoon. The surface and bottom water from the Morrerias (11 km), the Isla del Gallo (15 km) and Alejandria (17 km) sites, as well as the sediment samples from Isla del Gallo and Alejandria all plot in the second cluster. Additionally, the top layer of the sediment core, taken from between Isla del Gallo and Morrerias (at roughly 13 km) can be found in this cluster. These samples were all taken from locations after the large salinity increase where the system changes from a fluvial to a lagoonal system. Noticeably, the sediment sample from the Morrerias site is missing in this lagoonal cluster.

Lastly, a third cluster is plotted in Quadrant IV along the y-axis of the PCA and contains mostly fluvial samples. The associated GDGTs with the fluvial cluster are GDGT-1, GDGT-2, and the crenarchaeol isomer (Cren'). This cluster contains the surface and bottom water samples and the sediment samples of the Hidalgo (0km) and Bocobarra grande (7 km) sites. The sediment sample from the Morrerias site also plots in this cluster, although it was taken from a location with higher measured salinities.

Analysing the three clusters, a clear distinction is observed between fresh water and saline water sam-

ples, indicating a separation between fluvial and lagoonal sampling locations. With the water samples and sediment sample from the Morrerias site at the mouth of the lagoon, it can be determined that signature river GDGTs are being removed from the water column as the salinity increases. Separate in situ production in the lagoon (from 11 km) then results in the lagoonal samples having a different GDGT signature to the river samples.

In the stretch of water between 7 and 11 km the transitional zone between the river and lagoon is located. In this section the salinity increases from 1.52‰ to 6.62‰ in the surface water, and even to 7.99‰ in the bottom water. The decrease in total brGDGTs and isoGDGTs in the surface waters at this transitional section could be attributed to the loss of OM-mineral interactions, due to changes in ionic strength (Kirkels et al., 2020). With the GDGTs binding less strongly to mineral surfaces in more saline waters, they become more labile and are subjected to the OM degradation processes (Blattmann et al., 2019). The increase of total brGDGTs and isoGDGTs in the sediment layer from 11 km to 17 km in the transect, is assumed to be the result of lagoonal in situ produced GDGTs that sequester over a longer period of time. The POC samples in the water column only represent a short timescale, whereas the sediment samples cover a much longer one (Kirkels et al., 2020). As a result, the lagoonal GDGTs are not being measured in the water samples. However, they are being measured in the sediment samples, as these samples cover the entire year of GDGT production due to sequestering.

Another important observation is that the observed GDGTs in the water column and sediments do not directly come from the adjacent soils. The soil samples in Quadrant 1 are dominated by 5-methylated brGDGt, whereas the water and sediment samples have a preference for the 6-methylated brGDGTs. This is contrary to the findings in previous studies where lakes have high terrestrial soil input (eg. Damsté et al., 2009, Blaga et al., 2009).

The separation of the 5 and 6-methylated brGDGTs between soil samples and those taken from the water and sediments, indicate in situ brGDGT production in the water column and sediment layer (De Jonge, Stadnitskaia, et al., 2014 & J. Guo et al., 2020). The in situ brGDGT production strongly overwrites the soil derived brGDGTs in the aquatic systems. This could be accounted to the lack of precipitation in the area resulting in soil run-off (De Jonge, Stadnitskaia, et al., 2014). The samples were taken during the transition period between the wet and dry season and no precipitation had fallen during the sampling campaign. This reasoning would be similar to that of the FAs where terrestrial higher plant biomarkers were only present in the sediment layer. As the sediment samples capture a larger time frame than the water samples, which includes the entire wet season. However, that argument does not hold up for the GDGTs as the sediment samples would have to plot separately from the the fluvial and lagoonal clusters. The sediment samples would then also have to plot closer to the soil samples, as they would have a higher 5-methylated brGDGT abundance. As the sediment samples do not plot close to the soil samples, this observation then only strengthens the assumption of in situ production of brGDGTs being present in the water column.

When analysing the Methanogenesis ratio values (Eq. 3) a strong increase of methanogenic archaeal production occurs in the lagoon (Tab. 4). In the river sediments, an increase from 1.5 to 1.9 is observed, indicating low methanogenic presence in the fresh water section of the transect (Blaga et al., 2009). Methanogenesis values in the water column in the same fluvial section show an average of 2.5. This means that a larger methanogenic presence is measured in the water column compared to the sediments in the fluvial section. However, it is not a significantly large methanogenic influence. In the lagoon, from 11 km onwards, the values increase strongly to values between 6.2 and 45.8. These high values are indicative of a very strong methanogenic input.

In the deep waters at the Isla del Gallo sampling station the Methanogenesis ratio increases to a huge value of 293.5. The ratio indicates a very strong presence of methanogenic input. Which comes as no surprise because methanogens are predominantly found in anoxic environments (Thauer et al., 2008). During the sampling campaign, bottom water oxygen levels were not able to be measured at the Morrerias and Isla del Gallo locations (Tab. 1) due to presumed anoxia. Additionally, the bottom waters and sediment samples at these locations had strong sulphuric smells, which strengthend the

presumption of anoxia. Now with the large presence of GDGT-0 measured and therefore the presence of anoxic methanogens, our beliefs of anoxic bottom waters at the deeper parts of the Manialtepec lagoon are further strengthend.

4.2 Speculated carbon cycle in the Manialtepec estuary

Summarising the findings of the FA and GDGT concentrations and distribution across the lagoon, and combining those with the physical parameters, a speculation can be made on part of the OM cycle in the Manialtepec estuary. A schematic containing the major sources and sinks of OM is presented in Figure 12.

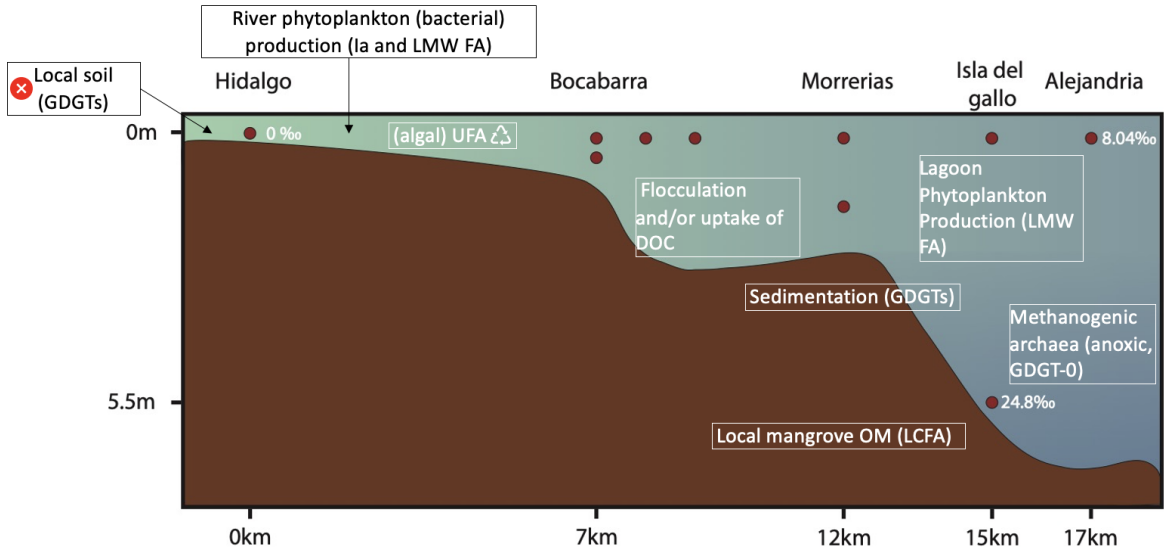

Figure 12: Schematic showing the the major processes of the OM cycle in the Manialtepec lagoon

In the fluvial section of the river between the Hidalgo and Bocobarra sampling stations, microbial primary production was observed. Bacteria derived brGDGTs (Ia) and LMW saturated FAs were distinctively present. Based on the lack of many unsaturated FAs, it is assumed that the microbial production in the river is predominantly driven by reworking of labile unsaturated FAs.

The finding of bacterial primary production is also supported by the distribution of brGDGT isomers. From the PCA (Fig. 11) we know the river samples contain a different chemical signature than the soil samples. Namely, the river samples show a preference to the 6-methylated brGDGTs (eg. IIa'), whereas the soil samples contain predominantly 5-methylated brGDGTs (eg. IIa). Additionally, this separation is also indicative of a lack of soil derived brGDGTs in the river and lagoon. The lack of soil run off could be due to a lack of precipitation during the sampling campaign, as that is one of the main causes of soil derived OM in aquatic systems.

Between Bocobarra and Morrerias the system changes from a fresh water fluvial to a saline water lagoonal environment. Paired with the salinity increase, a clear ecological environment change occurs. From the GDGT distribution of the PCA, the lagoonal samples distincly show another chemical signature compared to the fluvial samples. At this transitional point, the FA concentration increases significantly in SPM, and decreases in DOC, as a result of microbial production. These microbes include phytoplankton and archaea, as LMW FA and isoGDGT-0 were detected in the water column. Additionally, the fresh-salt water transition causes the river produced GDGTs to sequester and enter the sediment layer. The burial of these GDGTs in the sediment layer can act as a long term sink for OC.

Anoxic conditions are likely to be present at depth in the lagoon as the oxygen probe did not work

in the lagoonal bottom waters. A large spike of GDGT-0 was measured in the bottom waters at the Isla del Gallo. Using the GDGT-0 over crenarchaeol ratio, a strong methanogenic archaeal presence was determined here. Methanogens predominantly live under anoxic conditions, thus their presence confirms the presumed anoxia at depth.

Lastly, terrestrial derived FAs were only detected in the sediment layer and not in the DOC and SPM fractions of the water column. It is thought that these long chain FAs originate from leaf litter of local mangroves. The local transport is a consequence of low water velocity in the lagoon as well as the topography of the lagoon floor. Two potential causes of the lack of terrestrial FAs in the water column are reworking or degradation of the acids. However, it could be due to a difference in captured time frame of the samples. Where the water sample contains the molecules of the present time, the sediment layer also covers the past. Due to sedimentation and preservation of molecules in the sediment layer, these samples contain information about the entire year (wet and dry season). While the water samples only cover the period of the sampling campaign, which lacked precipitation.

5 Conclusion

To conclude, it was found that many different biogeochemical processes occur in the Manialtepec Lagoon influencing the composition and distribution of fatty acid and GDGT biomarkers. Biomarkers indicating microbial production were found abundantly in the water column and sediment layer. No terrestrial biomarkers were found in the water column as a result of reworking of the molecules or due to a of the lack of precipitation. High amounts of GDGT-0 indicated methanogen communities in the deep water of the lagoon.

In the sediment layer, terrestrial higher plant fatty acids were found, which were deposited there from local mangrove trees. At the fresh-salt water interface the river produced brGDGTs and isoGDGTs seem to sequester in the sediment layer, where they can be buried resulting in a long term carbon sink.

A salinity driven influence on the fate of OM in an estuary was not identified. From the biomarker analysis it became apparent that the composition and distribution of OM is driven by local ecological niches. However, with different FA and GDGT producing communities found in the fluvial and lagoonal section, it can be concluded that the change of salinity does have an effect on the ecological niches in the lagoon.

Finally, when looking at the transportation of OM through an estuary it is shown that terrestrial organic matter is heavily reworked in the water column before reaching the ocean. As a result, only small amounts of terrOM actually reach the ocean floor on continental shelves where it can be buried long term. A lot of the carbon from terrOM is either released back into the atmosphere as CO_2 or it is reworked by microbes. The OM that was initially from a terrestrial source will then be identified as OM from an aquatic source once it reaches the open ocean. Then, the OM that is eventually buried on the continental shelf is not detected as terrOM anymore.

Acknowledgements

First of all, I would like to send my sincere gratitude to my daily supervisor Pablo Martínez-Sosa. During my thesis Pablo guided and helped me enthusiastically and with great support. His enthusiasm and knowledge on the project motivated me greatly throughout the entire period. I am also so thankful that I could accompany him on the fieldwork campaign. In Mexico he acted as my personal tour guide and translator. He guided me on what to do, where to go, or what to eat. Also, many thanks to my supervisor and examiner Francien Peterse for guiding me through the project with great insights.

Secondly, I would like to thank Miguel Ángel Martínez-Carrillo, of the Universidad Nacional Autonóma de México (UNAM), for his support during the field campaign in Mexico, and for performing important ^{14}C analysis. Together with his wife Ana Maria Sosa Reyes they made me feel at home when in Mexico, for which I am very thankful.

In addition, I would like to thank Alejandra (Darla) Torres-Ariño and Vladislav Carnero Bravo, of the Universidad del Mar, Puerto Ángel, Oaxaca, for all their help during the fieldwork campaign. Whether it being giving us crucial information about the Manialtepec Lagoon, help collect the samples, or help process the core at their facilities. Also, many thanks to their students Mitzi Elizabeth Cruz Valdes, Oswaldo Alejandro Guerra Aldaz, Martha Constanza Tendilla Castellon, Esmeralda Pérez Ambrocio, Michelle Salinas Cabrera, and Diana Yurano Roque Castro for their help on the lagoon taking samples and processing the core at UMAR.

Furthermore, many thanks to Desmond Eefting, Mariska Hoorweg, Klaas Nierop, and John Visser for showing me the way around the organic geochemistry laboratory and performing important analysis on the samples. Also, in the laboratory at UNAM Corina Solís Rosales was of great importance for the ^{14}C measurements.

I would also like to thank everybody at the Earth Science department for creating a pleasant and fun work environment. Especially, many thanks to my friends in the department and fellow MSc students who were always available for a coffee break, or a brainstorming session.

Finally, my thanks and appreciation go to my family and friends who supported me throughout my studies. In particular my brother and mother. Both for proofreading my project, and my brother for always being available for computer related questions. With all your time and energy, during e.g. brainstorms and coffee breaks you helped me tremendously.

References

Ahlgren, G., Gustafsson, I.-B., & Boberg, M. (1992). Fatty acid content and chemical composition of freshwater microalgae 1. *Journal of phycology*, *28*(1), 37–50.

Anderson, T. R., Hawkins, E., & Jones, P. D. (2016). Co2, the greenhouse effect and global warming: From the pioneering work of arrhenius and callendar to today's earth system models. *Endeavour*, *40*(3), 178–187.

Arriola, P. (2021). The phenomenom of bioluminescence in puerto escondido [https://www.puerto-escondido.mx/en/2021/03/05/bioluminescence-in-puerto-escondido/ [Accessed: (05-03-2024)]].

Aufdenkampe, A. K., Mayorga, E., Raymond, P. A., Melack, J. M., Doney, S. C., Alin, S. R., Aalto, R. E., & Yoo, K. (2011). Riverine coupling of biogeochemical cycles between land, oceans, and atmosphere. *Frontiers in Ecology and the Environment*, *9*(1), 53–60.

Bauer, J. E., Cai, W.-J., Raymond, P. A., Bianchi, T. S., Hopkinson, C. S., & Regnier, P. A. (2013). The changing carbon cycle of the coastal ocean. *Nature*, *504*(7478), 61–70.

Baxter, A., Van Bree, L., Peterse, F., Hopmans, E., Villanueva, L., Verschuren, D., & Damsté, J. S. (2021). Seasonal and multi-annual variation in the abundance of isoprenoid gdgt membrane lipids and their producers in the water column of a meromictic equatorial crater lake (lake chala, east africa). *Quaternary Science Reviews*, *273*, 107263.

Blaga, C. I., Reichart, G.-J., Heiri, O., & Sinninghe Damsté, J. S. (2009). Tetraether membrane lipid distributions in water-column particulate matter and sediments: A study of 47 european lakes along a north–south transect. *Journal of Paleolimnology*, *41*, 523–540.

Blattmann, T. M., Liu, Z., Zhang, Y., Zhao, Y., Haghipour, N., Montluçon, D. B., Plötze, M., & Eglinton, T. I. (2019). Mineralogical control on the fate of continentally derived organic matter in the ocean. *Science*, *366*(6466), 742–745.

Blumenberg, M., Seifert, R., Reitner, J., Pape, T., & Michaelis, W. (2004). Membrane lipid patterns typify distinct anaerobic methanotrophic consortia. *Proceedings of the National Academy of Sciences*, *101*(30), 11111–11116.

Bouillon, S., Connolly, R., & Lee, S. (2008). Organic matter exchange and cycling in mangrove ecosystems: Recent insights from stable isotope studies. *Journal of sea research*, *59*(1-2), 44–58.

Brocks, J. J., Love, G. D., Summons, R. E., Knoll, A. H., Logan, G. A., & Bowden, S. A. (2005). Biomarker evidence for green and purple sulphur bacteria in a stratified palaeoproterozoic sea. *Nature*, *437*(7060), 866–870.

Budge, S. M., & Parrish, C. C. (1998). Lipid biogeochemistry of plankton, settling matter and sediments in trinity bay, newfoundland. ii. fatty acids. *Organic geochemistry*, *29*(5-7), 1547–1559.

Burdige, D. J. (2005). Burial of terrestrial organic matter in marine sediments: A re-assessment. *Global Biogeochemical Cycles*, *19*(4).

Canuel, E. A., & Hardison, A. K. (2016). Sources, ages, and alteration of organic matter in estuaries. *Annual review of marine science*, *8*, 409–34. https://api.semanticscholar.org/CorpusID:34130420

Carlson, C. A., Hansell, D. A., Nelson, N. B., Siegel, D. A., Smethie, W. M., Khatiwala, S., Meyers, M. M., & Halewood, E. (2010). Dissolved organic carbon export and subsequent remineralization in the mesopelagic and bathypelagic realms of the north atlantic basin. *Deep Sea Research Part II: Topical Studies in Oceanography*, *57*(16), 1433–1445.

Chappe, B., Michaelis, W., Albrecht, P., & Ourisson, G. (1979). Fossil evidence for a novel series of archaebacterial lipids. *Naturwissenschaften*, *66*, 522–523.

Chen, J., Gu, B., LeBoeuf, E. J., Pan, H., & Dai, S. (2002). Spectroscopic characterization of the structural and functional properties of natural organic matter fractions. *Chemosphere*, *48*(1), 59–68.

Cole, J. J., Prairie, Y. T., Caraco, N. F., McDowell, W. H., Tranvik, L. J., Striegl, R. G., Duarte, C. M., Kortelainen, P., Downing, J. A., Middelburg, J. J., et al. (2007). Plumbing the global carbon cycle: Integrating inland waters into the terrestrial carbon budget. *Ecosystems*, *10*, 172–185.

Contreras, F., Castañeda, O., & Torres, R. (1997). Hidrología, nutrientes y productividad primaria en las lagunas costeras del estado de oaxaca, méxico. *Hidrobiológica*, *7*(1), 9–17.

Dalsgaard, J., John, M. S., Kattner, G., Müller-Navarra, D., & Hagen, W. (2003). Fatty acid trophic markers in the pelagic marine environment.

Damsté, J. S. S., Ossebaar, J., Abbas, B., Schouten, S., & Verschuren, D. (2009). Fluxes and distribution of tetraether lipids in an equatorial african lake: Constraints on the application of the tex86 palaeothermometer and bit index in lacustrine settings. *Geochimica et Cosmochimica Acta*, *73*(14), 4232–4249.

Damsté, J. S. S., Schouten, S., Hopmans, E. C., Van Duin, A. C., & Geenevasen, J. A. (2002). Crenarchaeol. *Journal of lipid research*, *43*(10), 1641–1651.

De Jonge, C., Hopmans, E. C., Zell, C. I., Kim, J.-H., Schouten, S., & Damsté, J. S. S. (2014). Occurrence and abundance of 6-methyl branched glycerol dialkyl glycerol tetraethers in soils: Implications for palaeoclimate reconstruction. *Geochimica et Cosmochimica Acta*, *141*, 97–112.

De Jonge, C., Stadnitskaia, A., Hopmans, E. C., Cherkashov, G., Fedotov, A., & Damsté, J. S. S. (2014). In situ produced branched glycerol dialkyl glycerol tetraethers in suspended particulate matter from the yenisei river, eastern siberia. *Geochimica et Cosmochimica Acta*, *125*, 476–491.

De Rosa, M., & Gambacorta, A. (1988). The lipids of archaebacteria. *Progress in lipid research*, *27*(3), 153–175.

De Rosa, M., Gambacorta, A., Lanzotti, V., Trincone, A., Harris, J. E., & Grant, W. D. (1986). A range of ether core lipids from the methanogenic archaebacterium methanosarcina barkeri. *Biochimica et Biophysica Acta (BBA)-Lipids and Lipid Metabolism*, *875*(3), 487–492.

Derrien, M., Yang, L., & Hur, J. (2017). Lipid biomarkers and spectroscopic indices for identifying organic matter sources in aquatic environments: A review. *Water research*, *112*, 58–71.

Fang, J., Wu, F., Xiong, Y., Li, F., Du, X., An, D., & Wang, L. (2014). Source characterization of sedimentary organic matter using molecular and stable carbon isotopic composition of n-alkanes and fatty acids in sediment core from lake dianchi, china. *Science of the Total Environment*, *473*, 410–421.

Gao, J., Mikutta, R., Jansen, B., Guggenberger, G., Vogel, C., & Kalbitz, K. (2020). The multilayer model of soil mineral–organic interfaces—a review. *Journal of Plant Nutrition and Soil Science*, *183*(1), 27–41.

Gliozzi, A., Paoli, G., De Rosa, M., & Gambacorta, A. (1983). Effect of isoprenoid cyclization on the transition temperature of lipids in thermophilic archaebacteria. *Biochimica et Biophysica Acta (BBA)-Biomembranes*, *735*(2), 234–242.

Guo, J., Glendell, M., Meersmans, J., Kirkels, F., Middelburg, J. J., & Peterse, F. (2020). Assessing branched tetraether lipids as tracers of soil organic carbon transport through the carminowe creek catchment (southwest england). *Biogeosciences*, *17*(12), 3183–3201.

Guo, W., Jia, G., Ye, F., Xiao, H., & Zhang, Z. (2019). Lipid biomarkers in suspended particulate matter and surface sediments in the pearl river estuary, a subtropical estuary in southern china. *Science of the total environment*, *646*, 416–426.

Harwood, J., & Gurr, M. (2013). *Lipid biochemistry: An introduction*. Springer Science & Business Media.

Hedges, J. I., Keil, R. G., & Benner, R. (1997). What happens to terrestrial organic matter in the ocean? *Organic geochemistry*, *27*(5-6), 195–212.

Holtvoeth, J., Vogel, H., Wagner, B., & Wolff, G. (2010). Lipid biomarkers in holocene and glacial sediments from ancient lake ohrid (macedonia, albania). *Biogeosciences*, *7*(11), 3473–3489.

Hopmans, E. C., Schouten, S., & Damsté, J. S. S. (2016). The effect of improved chromatography on gdgt-based palaeoproxies. *Organic Geochemistry*, *93*, 1–6.

Hopmans, E. C., Weijers, J. W., Schefuß, E., Herfort, L., Damsté, J. S. S., & Schouten, S. (2004). A novel proxy for terrestrial organic matter in sediments based on branched and isoprenoid tetraether lipids. *Earth and Planetary Science Letters*, *224*(1-2), 107–116.

Jackson, R., Le Quéré, C., Andrew, R., Canadell, J., Peters, G., Roy, J., & Wu, L. (2017). Warning signs for stabilizing global co2 emissions. *Environmental Research Letters*, *12*(11), 110202.

Kida, M., & Fujitake, N. (2020). Organic carbon stabilization mechanisms in mangrove soils: A review. *Forests*, *11*(9), 981.

Kim, J.-H., Schouten, S., Hopmans, E. C., Donner, B., & Damsté, J. S. S. (2008). Global sediment core-top calibration of the tex86 paleothermometer in the ocean. *Geochimica et Cosmochimica Acta*, *72*(4), 1154–1173.

Kirkels, F. M., Zwart, H. M., Basu, S., Usman, M. O., & Peterse, F. (2020). Seasonal and spatial variability in δ18o and δd values in waters of the godavari river basin: Insights into hydrological processes. *Journal of Hydrology: Regional Studies*, *30*, 100706.

Kleber, M., Sollins, P., & Sutton, R. (2007). A conceptual model of organo-mineral interactions in soils: Self-assembly of organic molecular fragments into zonal structures on mineral surfaces. *Biogeochemistry*, *85*, 9–24.

Lee, C., Wakeham, S., & Arnosti, C. (2004). Particulate organic matter in the sea: The composition conundrum. *AMBIO: A Journal of the Human Environment*, *33*(8), 565–575.

Lowe, A. T., Galloway, A. W., Yeung, J. S., Dethier, M. N., & Duggins, D. O. (2014). Broad sampling and diverse biomarkers allow characterization of nearshore particulate organic matter. *Oikos*, *123*(11), 1341–1354.

Matsuda, H., & Koyama, T. (1977). Early diagenesis of fatty acids in lacustrine sediments—ii. a statistical approach to changes in fatty acid composition from recent sediments and some source materials. *Geochimica et Cosmochimica Acta*, *41*(12), 1825–1834.

Meyers, P. A., & Ishiwatari, R. (1993). Lacustrine organic geochemistry—an overview of indicators of organic matter sources and diagenesis in lake sediments. *Organic geochemistry*, *20*(7), 867–900.

Meziane, T., & Tsuchiya, M. (2000). Fatty acids as tracers of organic matter in the sediment and food web of a mangrove/intertidal flat ecosystem, okinawa, japan. *Marine Ecology Progress Series*, *200*, 49–57.

Middelburg, J. J., & Herman, P. M. (2007). Organic matter processing in tidal estuaries. *Marine Chemistry*, *106*(1-2), 127–147.

Napolitano, G. E. (1999). Fatty acids as trophic and chemical markers in freshwater ecosystems. *Lipids in freshwater ecosystems*, 21–44.

Nichols, P. D., Volkman, J. K., & Johns, R. (1983). Sterols and fatty acids of the marine unicellular alga, fcrg 51. *Phytochemistry*, *22*(6), 1447–1452.

Osterholz, H., Kirchman, D. L., Niggemann, J., & Dittmar, T. (2016). Environmental drivers of dissolved organic matter molecular composition in the delaware estuary. *Frontiers in Earth Science*, *4*, 95.

Parkes, R. J., & Taylor, J. (1983). The relationship between fatty acid distributions and bacterial respiratory types in contemporary marine sediments. *Estuarine, Coastal and Shelf Science*, *16*(2), 173–189.

Peters, K. E., Walters, C. C., & Moldowan, J. M. (2005). *The biomarker guide* (Vol. 1). Cambridge university press.

Pitcher, A., Hopmans, E. C., Mosier, A. C., Park, S.-J., Rhee, S.-K., Francis, C. A., Schouten, S., & Sinninghe Damsté, J. S. (2011). Core and intact polar glycerol dibiphytanyl glycerol tetraether lipids of ammonia-oxidizing archaea enriched from marine and estuarine sediments. *Applied and environmental microbiology*, *77*(10), 3468–3477.

Repasch, M., Scheingross, J. S., Hovius, N., Lupker, M., Wittmann, H., Haghipour, N., Gröcke, D. R., Orfeo, O., Eglinton, T. I., & Sachse, D. (2021). Fluvial organic carbon cycling regulated by sediment transit time and mineral protection. *Nature Geoscience*, *14*(11), 842–848.

Resmi, P., Gireeshkumar, T., Ratheesh Kumar, C., Udayakrishnan, P., & Chandramohanakumar, N. (2023). Distribution and sources of fatty acids in surface sediments of mangrove ecosystems in the northern kerala coast, india. *Environmental Forensics*, *24*(5-6), 183–196.

Rustan, A. C., & Drevon, C. A. (2001). Fatty acids: Structures and properties. *e LS*.

Sargent, J. (1987). Lipid biomarkers in marine ecology. *Microbes and the sea.*, 119–138.

Schouten, S., Hopmans, E. C., & Damsté, J. S. S. (2013). The organic geochemistry of glycerol dialkyl glycerol tetraether lipids: A review. *Organic geochemistry*, *54*, 19–61.

Schouten, S., Hopmans, E. C., Schefuß, E., & Damste, J. S. S. (2002). Distributional variations in marine crenarchaeotal membrane lipids: A new tool for reconstructing ancient sea water temperatures? *Earth and Planetary Science Letters*, *204*(1-2), 265–274.

Sinninghe Damsté, J., Pancost, R., Hopmans, E., & Party, M. S. S. (2001). Archaeal lipids in mediterranean cold seeps: Molecular proxies for anaerobic methane oxidation. *Geochimica et Cosmochimica Acta*, *65*(10), 1611–1627.

Summons, R. E., Welander, P. V., & Gold, D. A. (2022). Lipid biomarkers: Molecular tools for illuminating the history of microbial life. *Nature Reviews Microbiology*, *20*(3), 174–185.

Thauer, R. K., Kaster, A.-K., Seedorf, H., Buckel, W., & Hedderich, R. (2008). Methanogenic archaea: Ecologically relevant differences in energy conservation. *Nature Reviews Microbiology*, *6*(8), 579–591.

Tierney, J. E., Russell, J. M., Eggermont, H., Hopmans, E., Verschuren, D., & Damsté, J. S. (2010). Environmental controls on branched tetraether lipid distributions in tropical east african lake sediments. *Geochimica et Cosmochimica Acta*, *74*(17), 4902–4918.

Tierney, J. E., & Tingley, M. P. (2014). A bayesian, spatially-varying calibration model for the tex86 proxy. *Geochimica et Cosmochimica Acta*, *127*, 83–106.

Torres-Ariño, A., P´rez-P´rez, L. A., Rito-Ruíz, C. E., Luna-Hern´ndez, A., Velasco-Hern´ndez, M. D., Ramos-Espejel, L. I., & Herrera-Galindo, J. E. (2020). An´lysis de la coloracin en la laguna manialtepec, oaxaca, m´xico. *Ciencia y Mar*, *24*(70), 31–45.

Volkman, J., & Johns, R. (1977). The geochemical significance of positional isomers of unsaturated acids from an intertidal zone sediment. *Nature*, *267*(5613), 693–694.

Volkman, J., Johns, R., Gillan, F., Perry, G., & Bavor Jr, H. (1980). Microbial lipids of an intertidal sediment—i. fatty acids and hydrocarbons. *Geochimica et cosmochimica acta*, *44*(8), 1133–1143.

Wakeham, S. G. (1985). Wax esters and triacylglycerols in sinking particulate matter in the peru upwelling area (15 s, 75 w). *Marine chemistry*, *17*(3), 213–235.

Wang, Z., & Liu, W. (2012). Carbon chain length distribution in n-alkyl lipids: A process for evaluating source inputs to lake qinghai. *Organic Geochemistry*, *50*, 36–43.

Weijers, J. W., Schouten, S., Hopmans, E. C., Geenevasen, J. A., David, O. R., Coleman, J. M., Pancost, R. D., & Sinninghe Damsté, J. S. (2006). Membrane lipids of mesophilic anaerobic bacteria thriving in peats have typical archaeal traits. *Environmental Microbiology*, *8*(4), 648–657.

Weijers, J. W., Schouten, S., Spaargaren, O. C., & Damsté, J. S. S. (2006). Occurrence and distribution of tetraether membrane lipids in soils: Implications for the use of the tex86 proxy and the bit index. *Organic Geochemistry*, *37*(12), 1680–1693.

Weijers, J. W., Schouten, S., van den Donker, J. C., Hopmans, E. C., & Damsté, J. S. S. (2007). Environmental controls on bacterial tetraether membrane lipid distribution in soils. *Geochimica et Cosmochimica Acta*, *71*(3), 703–713.

Yoneyama, T., Okada, H., & Ando, S. (2010). Seasonal variations in natural 13c abundances in c3 and c4 plants collected in thailand and the philippines. *Soil Science & Plant Nutrition*, *56*(3), 422–426.